University of Pisa

Department of Information Engineering

Master's Thesis in
Telecommunication Engineering

Resource Allocation and Path Selection Strategies for Cognitive Radio Multihop Networks

Author:
Simone Scarfone

Supervisors:
Prof. Filippo Giannetti
Ing. Vincenzo Lottici
Ing. Paolo Del Fiorentino

June 21^{th}, 2016

Abstract

In the last years the world of communications, both research and industry, is heavily spending the energies on the fifth generation (5G) idea for wireless communications technology. Standards bodies have organized a schedule for a proposal of 5G standardization, which is expected to be in 2018, followed by a final specication around 2020 [1], [2]. With the coming of 5G, we will attend to the spatial densification of the cellular network, through heterogeneous architectures, i.e., small cells or a flexible combination of evolved existing technologies (3G, 4G, WiFi). For such a scenario, multihop communication could have an increasingly important part. In this thesis are proposed novel strategies of resource allocation (RA) and path selection (PS) for cognitive radio (CR) multihop communications over a packet-oriented and bit-interleaved-coded OFDM transmission, employing practical modulation and coding schemes. CR is a promising paradigm to achieve efficient use of the frequency spectrum by allowing the coexistence of both licensed (primary) and unlicensed (secondary) users together in the same bandwidth.

The performance of the system are evaluated in terms of goodput (GP), which is defined as the number of information bits delivered in error free packets per unit of time, and a local RA (L-RA) technique and a sub-optimal PS (Sub-PS) strategies are formulated for non-cooperative CR multihop communications. We tackle in particular the problem of to reduce the computational complexity and the signaling information over the feedback channel compared to the optimal solutions, called O-RA and O-PS respectively, and used as benchmark. We demonstrate with some new simulations that the the combination of L-RA and Sub-PS can effectively do it, paying a very little reduction of GP performance. An

additional PS solution is presented, called approximated Sub-PS (ASub-PS), which reduces the complexity further. For these simulations we use from one to five decode and-forward (DF) relay nodes (RNs) in different network configuration. Finally we have increased the number of RNs up to ten for to demonstrate that when number of relay grows the performance does not have a signicant improvement.

Contents

List of Acronyms

AGP	*Average GoodPut*
AMC	*Adaptive Modulation and Coding*
A-PGP	*Approximated Predicted GoodPut*
AWGN	*Additive With Gaussian Noise*
ARQ	*Automatic Repeat Request*
ASub-PS	*Approximated Sub-optimal Path Selection*
BER	*Bit Error Rate*
BIC	*Bit Interleaving Coding*
BS	*Base station*
CBS	*Coded Binary Symbols*
CC	*Convolutional Code*
CR	*Cognitive Radio*
CRC	*Cyclic Redundancy Check*
CSI	*Channel State Information*
DFT	*Discrete Fourier Transformer*
D2D	*Device to Device*
EGP	*Expected GoodPut*
ESM	*Effective SNR Mapping*
FFT	*Fast Fourier Transformer*
GP	*GoodPut*
IFFT	*Inverse Fast Fourier Transformer*
IoT	*Internet of Things*

LLR	*Log-Likelihood Ratio*
LOS	*Line of Sight*
LRA	*Link Resource Adaptation*
L-RA	*Local Resource Allocation*
LTE	*Long Term Evolution*
MCN	*Multihop Cellular Network*
MGF	*Moment Generating Function*
MIMO	*Multiple Input Multiple Output*
ML	*Maximum Likelihood*
NC	*Network Configuration*
OFDM	*Orthogonal Frequency Division Multiplexing*
OP	*Optimization Problem*
O-PS	*Optimal Path Selection*
O-RA	*Optimal Resource Allocation*
PA	*Power Allocation*
PER	*Packet Error Rate*
PGP	*Predicted GoodPut*
PHY	*Physical*
PU	*Primary User*
PDF	*Probability Density Function*
PS	*Path Selection*
PSD	*Power Spectral Density*
QAM	*Quadrature Amplitude Modulation*
QoS	*Quality of Service*
RA	*Resource Allocation*
RLC	*Radio Link Control*
RN	*Relay Node*
RS	*Relay Station*
RV	*Random Variable*
SISO	*Single Input Single Output*

SNR	*Signal to Noise Ratio*
SR	*Secondary User Receiver*
ST	*Secondary User Transmitter*
SU	*Secondary User*
Sub-PS	*Sub-optimal Path Selection*
SS	*Subscriber Station*
SSR	*Successive Set Reduction*
TM	*Transmission Mode*
UBA	*Uniform Bit Allocation*
UPA	*Uniform Power Allocation*
UWB	*Ultra Wide Band*

Introduction

In the current standard for wireless communication long term evolution (LTE) we can use two types of cellular network configuration. The first one is a conventional network in which a subscriber station (SS) is directly connect to a base station (BS). In the second type SS is connected to a BS through relay stations (RSs). In the latter case, we have a multihop cellular network (MCN) where the RSs cooperate to transmit information from SS to BS. In literature are present two different multihop communication setup: *cooperative* and *non-cooperative*. In the first, a source node sends information to the destination node exploiting more than one paths, one directly from the source and others through relay nodes [3], whereas in non-cooperative communication the destination node receives the message through a single path [4]. The possibility to use multihop wireless transmission in a 4G in order to improve coverage, data-rate or quality of service (QoS) [5], [6] is well studied in literature and an interesting article that describe how the relay technology is used in LTE standard is [7]. Now with the development of new multimedia applications and services, like streaming UHD, and the assimilation of the Internet of Things (IoT), we will attend to the spatial densification of the cellular network through heterogeneous architectures [8], and very high data rates transmission. Limitations and security issues [9] in 4G lead to the vision of new standard (5G) [10] that should be able to support communications for all special scenarios not supported by 4G networks

and multihop communications could have an increasingly important part [11]. Already many studies and system designs have been made to exploit the potential advantages of multihop and have resulted in several architectures, protocols, and analytical models in particular for (MCNs) [12],[13]. An example of MCN with relays for to extend the coverage or to increase the capacity within the cell is show in Figure 1.1. When we have a network with more RSs and so many possible paths between SS and BS, therefore routing and resource allocation are the typical problems. Many papers have been published for to address these problems and present several solutions for MCN cooperative and non-cooperative. Usually, the metrics for evaluate the performance of the network are the throughput or the capacity. For example some significant results are in work [14] where an optimal RA solution for cooperative orthogonal frequency division multiplexing access (OFDMA) multihop networks is presented, in which a centralized network controller maximizes the minimum throughput among all nodes. In [15], the authors consider a non-cooperative OFDM multihop link where the RA is based on the outage probability minimization. An interesting paper is [16], which presents a path selection (PS) strategy for CR multihop networks. This PS method provides an unlicensed user with the route which has the lowest probability of interfering with the licensed users. An optimal power allocation (PA) for MIMO multihop cooperative transmissions is presented in [17], where the end-to-end achievable rate is maximized. Moreover, in [18] a PA and a PS strategy are presented that minimizes an approximate expression of the overall BER. The authors also make a comparison between the BER of non-cooperative and cooperative multi-hop networks. In many works, as in [19], the RA strategy is for dual-hop transmissions. An interesting case of dual-hop communication is the Device-to-Device (D2D) transmission that allow nearby devices to establish local links so that traffic

ows directly between them, instead of through the base station and a particular case is the D2D relay for traffic offloading, where an user with a better geometry than a base station acts as a relay for another nearby user [20],[21]. In this thesis we consider a cognitive radio (CR) multihop scenario with more than two relay and modified RA method of [19] and PS criterion presented in [18]. In particular, in [18] the PS strategy has been evaluated for a single carrier system while here we have a multi-carrier transmission. In detail we present a local RA (L-RA) technique and a sub-optimal PS (Sub-PS) strategy for non-cooperative CR multihop communications, in which the intermediate nodes transmit packets, using a DF protocol with a BIC-OFDM modulation [22]. Optimal solutions for RA and PS, called O-RA and O-PS respectively, will be used as benchmark. The O-RA and O-PS are derived from [19], extending the solution from a dual-hop to a multihop transmission. In particular, O-PS provides the optimal path through an exhaustive search, which results in a polynomial complexity depending on the number M of RNs of the network. The Sub-PS, instead, has a complexity of $\mathcal{O}(M^3)$. We will show that the L-RA and Sub-PS are able to reduce the signaling over the feedback channel and the computational complexity compared to the O-RA with O-PS method, while paying only a small penalty in terms of GP performance The performance of the system are evaluated in terms of goodput (GP), which is a more suitable metric to quantify the actual performance of packet-oriented systems respect to the capacity [22]. In order to optimize the GP, the transmitter must know the channel state, but in a realistic wireless networks, there are errors in the channel estimation and a delay over the feedback channel. Thus the channel state information (CSI) will not be perfect and therefore any transmitting node only will have outdated and imperfect CSI. Consequently in this work we exploit a prediction of the GP, i.e. PGP as a performance metric [23].

An additional PS solution will be presented, called approximated Sub-PS (ASub-PS), which is able to reduce the computational complexity to $\mathcal{O}(M^2)$, without showing a signicant GP performance loss. Sub-PS and ASub-PS do not require information about the network topology and the coordinates of the source and destination and thus reduce the signaling over the feedback channel compared with the O-PS method. The effectiveness of the L-RA, Sub-PS and ASub-PS algorithms are corroborated by extensive simulation results over a ITU multipath channel for various network setups. Finally we evaluate whether the increase of the number of relay corresponds to a performance increase.

Chapter 1

Multihop Cognitive Radio Scenario

1.1 Cognitive Radio Scenario

The cognitive radio (CR) network is an innovative software defined radio technique considered to be one of the promising technologies to improve the utilization of the congested RF spectrum [24]. Adopting CR is motivated by the fact that a large portion of the radio spectrum is underutilized most of the time. In CR networks, a secondary system can share spectrum bands with the licensed primary system, either on an interference-free basis or on an interference-tolerant basis [24]. The CR technique is considered, because it is a possible solution to increase the overall spectral efficiency by allowing additional users in an already crowded spectrum. The CR network should be aware of the surrounding radio environment and regulate its transmission accordingly.

Depending on the knowledge that is needed to coexist with the primary network, cognitive radio approaches fall into two classes:

- *interference-free CR networks*

- *interference-tolerant CR networks*

In interference-free CR networks, CR users are allowed to borrow spectrum resources only when licensed users do not use them. A key to enabling interference-free CR networks is figuring out how to detect the spectrum holes (white space) that spread out in wideband frequency spectrum. CR receivers should first monitor and allocate the unused spectrum via spectrum sensing (or combining with geolocation databases) and feed this information back to the CR transmitter. A coordinating mechanism is required in multiple CR networks that try to access the same spectrum to prevent users colliding when accessing the matching spectrum holes. In interference-tolerant CR networks, CR users can share the spectrum resource with a licensed system while keeping the interference below a threshold. In comparison with interference-free CR networks, interference-tolerant CR networks can achieve enhanced spectrum utilization by opportunistically sharing the radio spectrum resources with licensed users, as well as better spectral and energy efficiency. It has been shown that the performance of CR systems can be very sensitive to any slight change in user densities, interference threshold, and transmission behaviors of the licensed system. This fact is illustrated in Figure 1.2, where we notice that the spectral efficiency decreases quickly with the increase in the number of primary receivers. However, the spectral efficiency can be improved by either relaxing the interference threshold of the primary system or considering only the CR users who have short distances to the secondary BS. In [25], hybrid CR networks have been proposed for adoption in cellular networks to explore additional bands and expand the capacity.

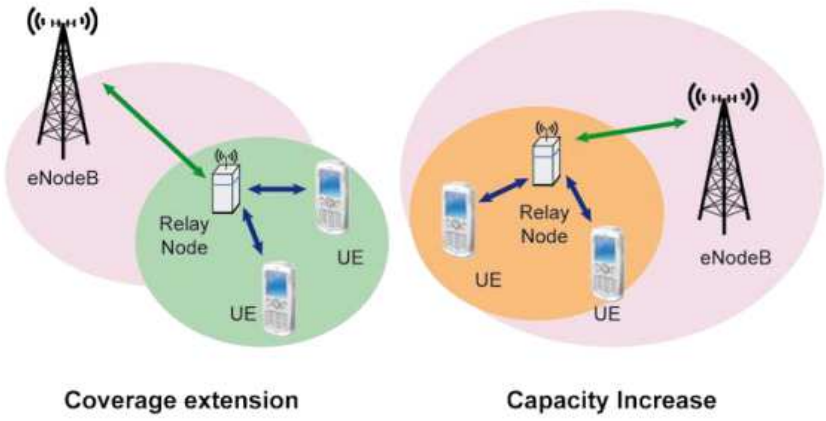

Figure 1.1: Example of multihop network

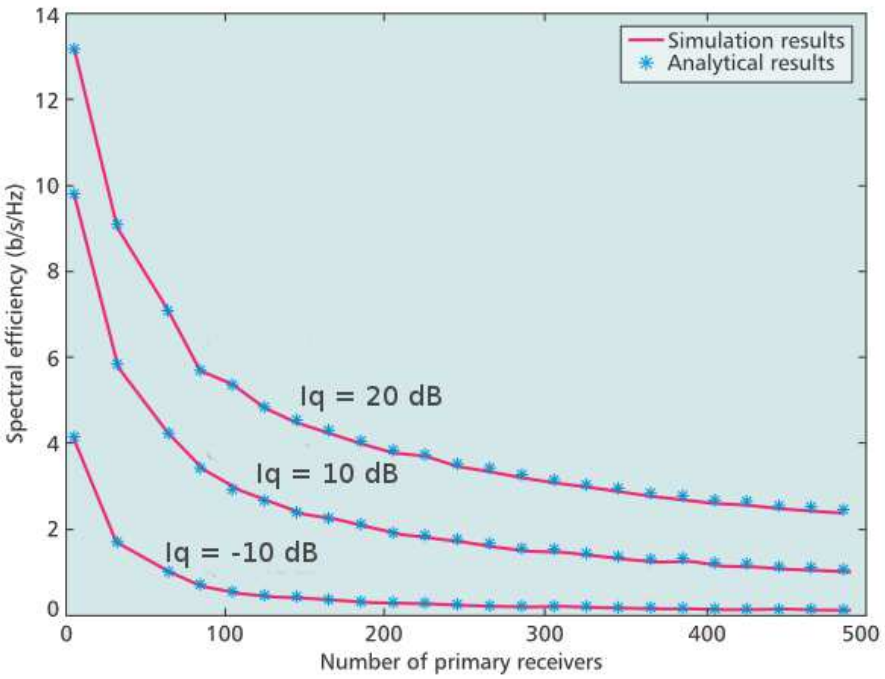

Figure 1.2: The average system spectral efficiency of a CR network as a function of the number of primary receivers (Q) with different values of interference thresholds I_q (number of secondary receivers = 20)

A major issue in interference-tolerant CR networks in 5G is how to reliably and practically manage the mutual interference of CR and primary systems. Regulating the transmit power is essential for the CR system to coexist with other licensed systems. An interference temperature model is introduced for this purpose to characterize the interference from the CR to the licensed networks. Interference cancellation techniques should also be applied to mitigate the interference at CR receivers. Another issue in interference-tolerant CR networks is that a feed-back mechanism is important to periodically inform the CR network about the "current" interference status at the licensed system. A practical solution is that the interference state information can be sent from licensed systems and collected by a central unit (or a third party system). Any CR network should first register to the central unit in order to be updated regarding the allowed spectrum and interference. Alternatively, the CR transmitters can listen to beacon signals transmitted from the primary receivers and rely on the channel reciprocity to estimate the channel coefficient. In this case, the CR transmitters can cooperate among themselves to regulate the transmit power and prevent the interference at the primary receivers being above the threshold. All these aspects define three main cognitive radio network paradigms *interweave*, *overlay* and *underlay*.

The interweave systems based on the original motivation of cognitive radio [26]. The secondary user (SU) detect the absence of PU signals in space, time, or frequency, and opportunistically communicate during these absences. The idea came about after studies conducted by the FCC [27], universities [28], and industry [29] showed that a major part of the spectrum is not fully utilized most of the time. In other words, there exist temporary space-time-frequency voids, referred to as spectrum holes or white spaces, that are not in constant use in both the licensed and unlicensed bands, as shown in Figure 1.3. Spectral holes can be exploited

by SU to operate in orthogonal dimensions of space, time or frequency relative to the primary user signals. Thus, the utilization of spectrum is improved by opportunistic reuse over the spectrum holes. The interweave technique requires detection of primary (licensed or unlicensed) users in one or more of the space-time-frequency dimensions. This detection is quite challenging since primary user activity changes over time and also depends on geographical location.

The premise for overlay systems, illustrated in Figure 1.4, is that the secondary transmitter has knowledge of the primary users transmitted data sequence (also called its *message*) and how this sequence is encoded (also called its *codebook*). Similar ideas apply when there are multiple secondary and primary users. The codebook information could be obtained, for example, if the primary users follow a uniform standard for communication based on a publicized codebook. Alternatively, the PUs could broadcast their codebooks periodically. In other words, in overlay systems the SU overhear the transmissions of the primary users, then use this information along with sophisticated signal processing and coding techniques to maintain or improve the performance of primary users, while also obtaining some additional bandwidth for their own communication. Under ideal conditions, sophisticated encoding and decoding strategies allow both the secondary and primary users to remove all or part of the interference caused by other users.

The underlay paradigm allows SU to operate if the interference they cause to PU is below a given threshold or meets a given bound on primary user performance degradation. Therefore in the underlay paradigm, rather than determining the exact interference it causes, a SU spread its signal over a very wide bandwidth such that the interference power spectral density is below the noise floor at any PU location (Figure 1.5). These spread signals are then despread at each of their intended sec-

ondary receivers. This spreading technique is the basis of both spread spectrum and ultrawideband (UWB) communications [30]. Alternatively, the secondary transmitter can be very conservative in its output power to ensure that its signal remains below the prescribed interference threshold. In this case, since the interference constraints in underlay systems are typically quite restrictive, this limits the SU to short range communications. Both spreading and severe restriction of transmit power avoid exact calculation of SU interference at primary receivers, instead using a conservative design whereby the collective interference of all secondary transmissions is small everywhere. This collective interference, sometimes called the interference temperature. In Figure 1.6 the interference toward the PU is represented in green. In this work we assume this underlay approach and in order to satisfy these constraints about the tolerable interference threshold, the transmitters of the secondary user network adapt their transmit power according to a dynamic resource allocation algorithm [31], [32]. These algorithms require the availability of CSI at the transmitting node. In most wireless networks, because of channel estimation errors and channel feedback delay, this CSI will not be perfect!

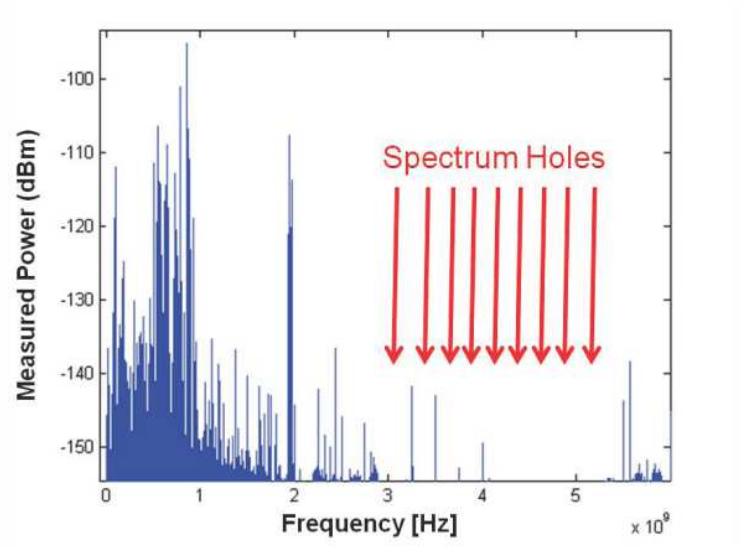

Figure 1.3: Spectral occupancy measurements up to 6 GHz in an urban area at mid-day (Berkeley Wireless Research Center (BWRC) [28]).

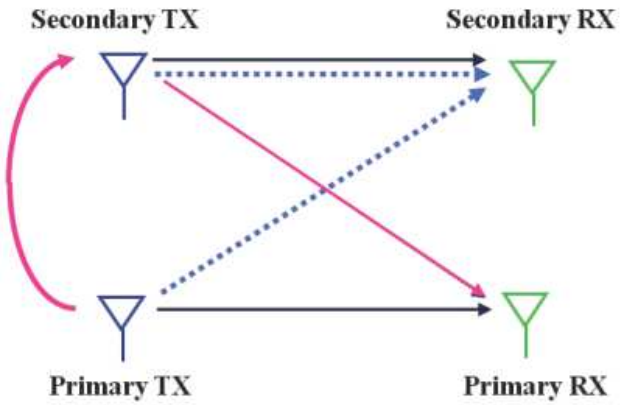

Figure 1.4: The overlay paradigm

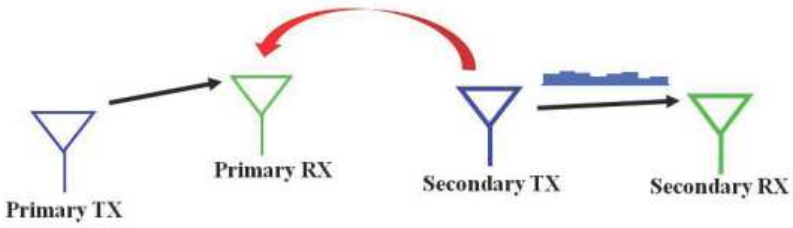

Figure 1.5: The underlay paradigm: wideband signaling (e.g. spread spectrum)

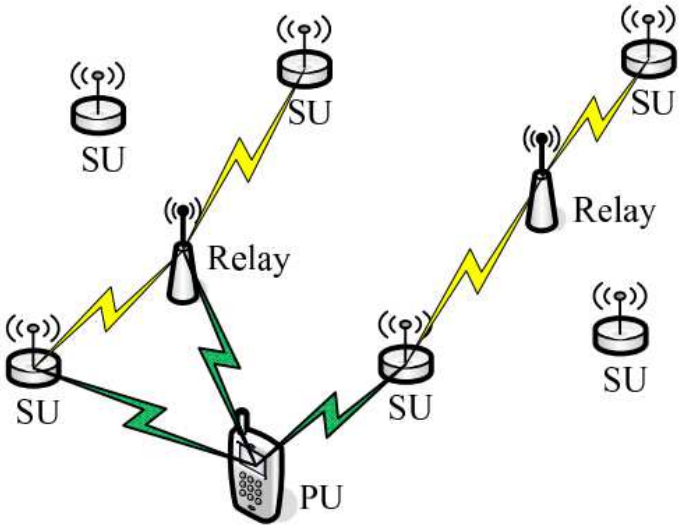

Figure 1.6: Example of interference toward PU in CR network

1.2 Multihop with Decode-and-Forward Relays

The next-generation cellular wireless networks will support high data rates and provide quality of service (QoS) for multimedia applications

with increased network capacity. Under limited frequency resources, the conventional approach to increase network capacity is to install more base stations to exploit spatial reuse. This solution is not very efficient because the cost of the BS transceiver is quite high. An alternative approach is to employ relay stations as intermediate nodes to establish multihop communication paths between mobile hosts and their corresponding BSs. So this approach leads to a multihop cellular network. MCNs have experienced a strong growth in recent years. An example of MCN with relays for to extend the coverage or to increase the capacity within the cell is show in Figure 1.1. A number of different architectures, protocols, and analytical models for MCNs have been proposed in the literature where different system aspects were investigated. There are two different type of MCN *cooperative* and *non-cooperative*. The main difference is that in cooperative the source node sent an information at the destination through diverse path, one directly from the source, whereas in non cooperative the destination node receives the message through a single path. Most common relaying strategies are or decode-and-forward (DF) or amplify-and-forward (AF). While a DF relay decodes, re-modulates and retransmit the received signal, an AF one simply amplifies and retransmit the signal without decoding. Compared to an AF relay, the complexity of a DF one is significantly higher due to its full processing capability. The DF protocol also requires a sophisticated media access control layer, which is unnecessary in the AF protocol. Overall, a DF relay is nearly as complex as a base station but some studies shows that DF protocol is better. For example the study in [33] shows that the outage probability in multihop relay channels is higher under the AF protocol, which automatically transforms into smaller outage capacity. Therefore, one has to conclude that while the AF protocol is better for uncoded systems (where the error propagation effect outweighs the noise

amplification), the opposite is true for systems using powerful capacity-approaching codes [34] as in this thesis. Thus the relay nodes will be DF. Because between ST and SR there are M fixed RNs the transmission of a data message always occurs in $N_{\mathrm{TS}} \leq M+1$ time slots (TSs), simply called links, which are assumed with different duration. $L = N_{\mathrm{TS}} - 1$ is the number of exploited RNs for the transmission. Below, we define the notation to define a generic path to connect the ST to the SR:

1. $\mathcal{P}(\mathrm{ST}, \mathrm{R}_{i_1}, \cdots, \mathrm{R}_{i_L}, \mathrm{SR})$ is the path connecting ST to SR passing through the $\mathrm{R}_{i_1}, \ldots, \mathrm{R}_{i_L}$ with $0 \leq L \leq M$, $i_1, ..., i_L \in \{1, ..., M\}$, and $i_j \neq i_k \forall j \neq k \in \{1, ..., L\}$;

2. $l \in \mathcal{L} \triangleq \{0, \cdots L\}$ is the generic link, $l = 0$ is the link ST-R_{i_1} and $l = L$ is the link R_{i_L}-SR.

Figure 1.7 shows an example of non-cooperative CR network, where the blu line indicates the selected path to transmit the information packet. Finally, the secondary user (SU) network consist of:

1. SU transmitter and receiver in underlay fashion;

2. M fixed DF relay nodes;

3. Q primary user

4. BIC-OFDM modulation

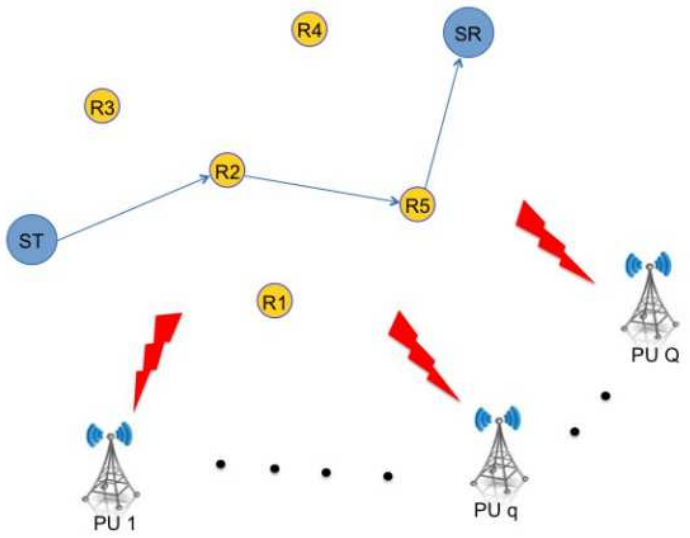

Figure 1.7: Example of CR non-cooperative multihop network, $M = 5$, $N_{\mathrm{TS}} = 3$, $L = 2$

1.3 BIC-OFDM

Multicarrier system have been proposed as a solution to channel variations. In this system the available bandwidth is divided into several subchannel or subcarrier. Each subcarrier experiences flat fading and therefore simple equalization techniques are applicable. If the channel bandwidth and transmission parameters are chosen properly, each subcarrier will be orthogonal to other subcarriers and we have a OFDM system. OFDM is usually combined with binary coding and the combination is referred to as bit interleaved coded OFDM (BIC-OFDM). BIC-OFDM is used in many standard like the 3GPP Long Term Evolution (LTE) wireless cellular systems.

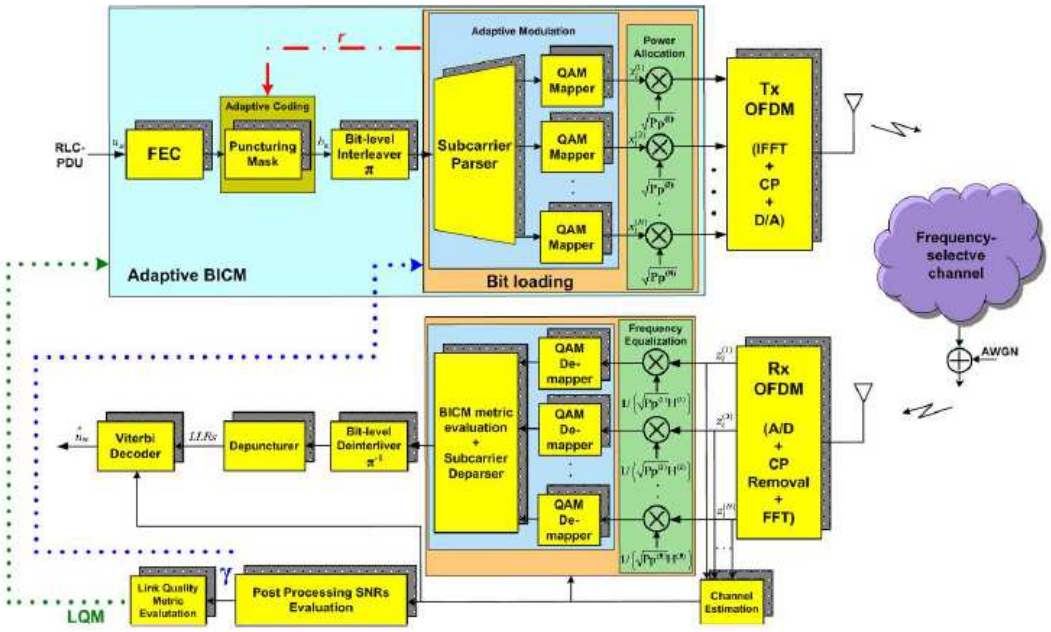

Figure 1.8: *SISO-BIC-OFDM System Model*

The block diagram of the single-input single-output (SISO) BIC-OFDM transceiver system is shown in Figure 1.8.

On the transmitter side, each packet is one to one mapped to a Radio Link Control sub-layer Protocol Data Unit (RLC-PDU) made of $N_{\mathrm{u}} = N_{\mathrm{h}} + N_{\mathrm{p}} + N_{\mathrm{CRC}}$ bits where N_{h}, N_{p} and N_{CRC} are the header, the payload and the CRC section respectively. Than it is transmitted through Φ consecutive OFDM symbols, which form an OFDM frame. All the OFDM symbols, belonging to the same frame (or block), experience the same fading realization. Each RLC-PDU is processed in two steps:

- *packet processing*
- *frame processing*

In the packet processing step, the RLC-PDU is input to the channel

encoder. For our channel encoding, we employ convolutional codes. The N_{u} bits are encoded by a convolutional coder, then punctured to obtain a certain code rate r. The code rate r is chosen in the set of punctured rates $D_r \triangleq \{r_0, \cdots, r_{\max}\}$, where r_0 is the mother code rate and $r_{\max}$ the minimum code rate. The resulting block consist of $N_{\mathrm{c}} = N_{\mathrm{u}}/r$ coded binary symbols (CBS) b_k, which are subsequently randomly interleaved. Interleaving is an important part of BIC because it guarantees the nearby bits from convolutional encoder to be separated over different fading samples. Therefore, nearby bits experience different fading gains and thus the diversity present in the channel can be exploited during decoding at the receiver. The bit-level interleaver randomly maps the generic cbs b_k, onto one of the label bits, carried by the symbols of the OFDM subcarriers, according to the follow notation:

$$b_k \rightarrow c_{\Pi(k)}, \tag{1.1}$$

$\Pi(k) \triangleq \{\varphi_k, n_k, i_k\}$ is the interleaver law, which maps the index k of the CBS into a set of three coordinates:

1. φ_k, the position of the OFDM symbol within the frame;
2. n_k, the OFDM subcarrier number;
3. i_k, the position of the cbs within the label of the QAM symbol on a certain subcarrier.

The interleaver is assumed to be fully random, so that the probability of mapping the generic cbd b_k - into the i-th label bit of the QAM symbol transmitted on the n-th subcarrier into the φ-th OFDM block - denoted as $c_{\varphi,n,i,}$ with $\varphi = 1, \ldots, \Phi$, $n = 1, \ldots, N$ and i $= 1, \ldots, m^{(n)}$, is

$$\Pr\{b_k \rightarrow c_{\varphi,n,i}\} \triangleq \frac{1}{Nc} \tag{1.2}$$

In the next frame processing that follows, the coded information in mapped onto the physical resources available in the time-frequency grid. With m_n denotes the number of CBS, allocated on the n-th subcarrier. In detail, the interleaved sequence of CBS is broken into subsequences of m_n bits each, which are Gray mapped onto the unit-energy symbols $x_n \in 2^{m_n}$-QAM constellation, with $m_n \in D_m = \{2, 4, 6\}$. This means that the index k of CBS b_k is one-to-one mapped into a set of two coordinates (i_k, n_k), that is, b_k occupies the i_kth position within the label of the 2^{m_n}-QAM symbol sent on the n_k subcarrier. The modulation symbols are re-arranged into the vector $\mathbf{x} \triangleq [x_1, \cdots, x_N]$ and allocated over the N available subcarriers along with a certain amount of power $\mathbf{P} \triangleq [\mathrm{P}_1, \cdots, \mathrm{P}_N]$, where P_n denotes the power load over the nth subcarrier, and satysfing:

$$\sum_{n=1}^{N} P_n \leq P \tag{1.3}$$

with P the available power in transmission. The process of power and bits distribution (among the subcarriers with a certain criterion) is called *Bit loading*. At this point, the data-bearing QAM symbols are transmitted, after having been subjected to the digital OFDM processing, including:

- IFFT with length N_{FFT};
- addiction of cyclic prefix (CP);
- Digital to Analog (D/A) conversion.

Then, the obtained signal is up-converted at carrier frequency f_c and transmitted over a frequency selected channel. The channel will be assumed stationary for whole frame duration. The duration in the time-domain of an OFDM symbol is equal to $T_{\mathrm{s}} \triangleq (N_{\mathrm{FFT}} + N_g)T$, where N_g is the length of the CP and T is the sample time in output at the OFDM transmission block.

At the receiver side, the signal will go through the whole inverse OFDM processing, in order to be coherently demodulated, subcarrier per subcarrier, exploiting the channel estimation, which will be assumed perfect. So the signal passes trough:

- the analogic-to-digital converter;
- the CP removal;
- the serial-to-parallel (S/P) converter.

The resulting signal samples are input to the discrete Fourier Transformer (DFT) block. The model of the signal samples at the output of the DFT block results:

$$z_n = \sqrt{P_n} x_n h_n + w_n, \tag{1.4}$$

where

- h_n is the complex-valued channel coefficient on subcarrier n, that is obtained as the nth coefficient of the DFT of the channel response (1.8), encompassing also the transmitter and receiver filter;
- $w_n \in \mathcal{CN}(0,\, \sigma_w^2)$ is the circular-symmetric complex-Gaussian random variable with standard deviation σ_w, denoting the thermal noise sample on subcarrier n.

The instantaneous post processing SNR values are then defined as

$$\gamma_n = P_n \frac{|h_n|^2}{\sigma_w^2}, \tag{1.5}$$

This post-processing SNRs are used for the BICM metric evaluation and for the Viterbi decoding. They are also used for making Link Adaptation at the next packet transmission. Finally, the soft-demodulated metrics are deinterlived and the Log-Likelihood Ratios (LLRs) will feed

a Viterbi decoder, in order to obtain a Maximum Likelihood (ML) estimation of the information bits, $\hat{u}_k$, composing the RLC-PDU. In particular, the soft metric of the kth coded binary symbol at the input of the decoder is expressed by:

$$\Lambda_k = \log \frac{\sum_{\tilde{x} \in \chi_{b'_k}^{(i_k,n_k)}} p\left(z_{n_k} | x_{n_k} = \tilde{x}, \gamma_{1,\cdots,N}\right)}{\sum_{\tilde{x} \in \chi_{b_k}^{(i_k,n_k)}} p\left(z_{n_k} | x_{n_k} = \tilde{x}, \gamma_{1,\cdots,N}\right)} \tag{1.6}$$

where

$$p\left(z_{n_k} | x_{n_k} = \tilde{x}, \gamma_{1,\cdots,N}\right) \propto \exp\left(-\left|z_{n_k} - \sqrt{\gamma_{n_k}}\tilde{x}\right|^2\right) \tag{1.7}$$

is the Gaussian-shaped probability density function (p.d.f.) of the received sample value, conditioned on the transmitted symbol $\tilde{x}$ and on $\gamma_{1,\cdots,N}$, $\chi_a^{(i,n)}$ represents the subset of all symbols belonging to the modulation adopted on the nth subcarrier whose ith label bit is equal to a and b'_k denotes the complement of bit b_k.

1.4 Channel Prediction Model

In a mobile-radio scenario, signals experience several degradation factors due to reflection, diffraction, scattering and, in general, to any obstacle that obstruct the line-of-sight (LOS) between transmitter and receiver. This phenomenon is called *multipath fading* (Figure 1.9). As a result, the receiver sees the superposition of multiple copies of the transmitted signal, each traversing a different path. Each signal copy will experience differences in attenuation, delay and phase shift while traveling from the source to the receiver. This can result in either constructive or destructive interference, amplifying or attenuating the signal power seen at the receiver. Moreover, another significant effect is the time variation in the structure of the medium. As a results, the characteristics of the paths

experienced by the transmitted signal can vary during time [35]. Statistical models for the channel impulse response of a fading multipath channel have been described in literature over the past years [36].

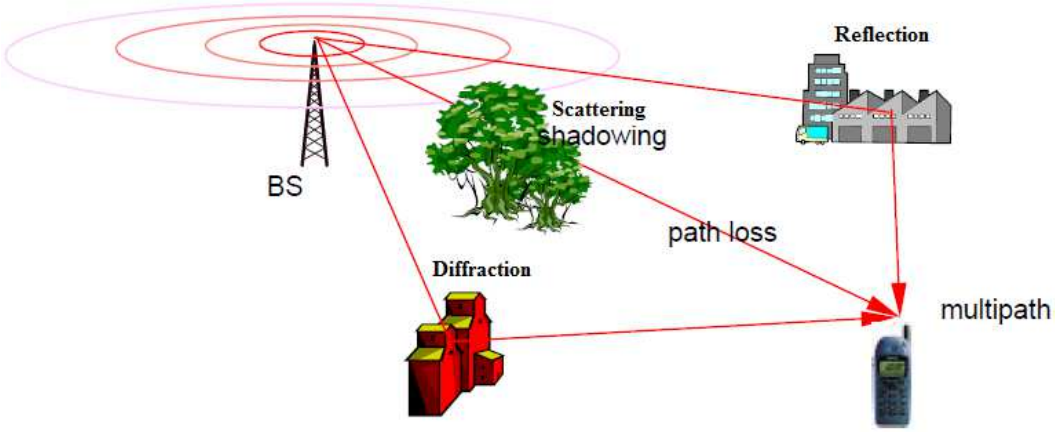

Figure 1.9: Multipath scenario

For our scenario we modeled the fading problem with the Rayleigh distribution. It is well known that a Rayleigh fading process is characterized by its power spectral density and its auto-correlation function.The auto-correlation function depends on the Doppler frequency which corresponds to the relative motion of the receiver and transmitter. In particular we have a Rayleigh fading (or small scale fading) if the multiple reflective paths are large in number and there is no line of sight signal component, hence the envelope of the received signal is statistically described by a Rayleigh probability density function (pdf).

We assume that the wireless channel between any two nodes of the SU network is a frequency-selective multipath fading channel with a correlation time that is much longer than the OFDM symbol duration T_s, so that the complex path gains can be considered constant over an interval T_s. Considering root-raised-cosine transmit and receive filters with

roll-off factor β [37], the impulse response $h_v(i)$ of the cascade of the transmit filter, the wireless channel and the receive filter, related to the ith OFDM symbol, is expressed as

$$h_v(i) = \sum_{\xi=0}^{\Xi} c_\xi(i) g(v - \tau_\xi) \tag{1.8}$$

where $c_\xi(i)$ and τ_ξ denote the gain and delay of the ξth path, and *g(v)* is a raised-cosine pulse with roll-off factor β. We assume that $h_v(i) = 0$ for $v < 0$ and for $v > \nu$, which is achieved by adding to all path delays a sufficiently large common delay to make $h_v(i)$ causal, and by taking ν sufficiently large. The gains of the different paths are independent zero-mean circularly symmetric CGRVs. According to Jakes model [38], where the power spectral density $S(f)$, also call DSP of Jakes, of the received signal is:

$$S(f) = \frac{\sigma_v^2}{\pi f_d} \frac{1}{\sqrt{1 - \left(\frac{f}{f_d}\right)}} \tag{1.9}$$

for $-f_d \leq f \leq f_d$ and the relative autocorrelated function computing the inverse Fourier transform of eq.(1.9) is

$$\mathrm{E}\left\{h_v(i+m) h_v^*(i)\right\} \triangleq \mathrm{J}_0(2\pi f_d m T_s) \sigma_v^2 \tag{1.10}$$

where $\mathrm{J}_0(\mathrm{x})$ represents the zeroth-order Bessel function of the first kind, and f_d denotes the Doppler spread.

For later use, we define $\mathbf{R}_c = \mathrm{diag}(\sigma_0^2, ..., \sigma_L^2)$ and the vector $\mathbf{h}(i) \triangleq [h_0(i), \ldots, h_\nu(i)]^T \in \mathbb{C}^{(\nu+1)\times 1}$ containing the $\nu+1$ samples of $h_v(i)$, given by

$$\mathbf{h}(i) \stackrel{\triangle}{=} \mathbf{G}\mathbf{c}(i) \tag{1.11}$$

where $c(i) \stackrel{\triangle}{=} [c_0(i), ..., c_\xi(i)]^T$ and $\mathbf{G}$ is the $(\nu+1)(\Xi+1)$ matrix with entries $\mathbf{G}_{k,\xi} \stackrel{\triangle}{=} g(kT - \tau_\xi)$, for $k = 0, \ldots, \nu$ and $\xi = 0, \ldots, \Xi$.

The corresponding frequency response is given by

$$\mathbf{H}(i) = \mathbf{F}\mathbf{h}(i) = [H_1(i), \ldots, H_N(i)]^T \tag{1.12}$$

where the Fourier matrix $\mathbf{F} \in \mathbb{C}^{N_{FFT} \times (\nu+1)}$ is determined by

$$\mathbf{F}_{n,u} \triangleq e^{-j2\pi(n-1)(u-1)/N_{FFT}}, \quad n = 0, ..., N_{FFT}; \quad u = 0, ..., \nu + 1.$$

The nth component of $\mathbf{H}(i)$ denotes the channel gain seen by the kth subcarrier in the ith OFDM symbol. In order to perform dynamic resource allocation, the transmitting nodes need some form of CSI. Therefore we assume that the transmitting node obtains the estimated impulse response from the corresponding receiving node via a feedback channel. If the transmitting node sends known pilot symbols, the receiving node is able to obtain a noisy version $\hat{\mathbf{H}}(i)$ of the frequency response $\tilde{\mathbf{H}}(i)$, i.e.,

$$\tilde{\mathbf{H}}(i) \triangleq \mathbf{H}(i) + \tilde{\mathbf{e}}(i), \tag{1.13}$$

where $\tilde{\mathbf{e}}(i) \sim \mathcal{CN}(0, \sigma_{\mathrm{e}}^2 \mathbf{I}_N)$ and $\sigma_{\mathrm{e}}^2 \triangleq \mathrm{E}\{|\tilde{e}_n|^2\} \cong \sigma_w^2 / P_{\mathrm{p}}$ $\forall n \in \mathcal{N}$. We denote by P_{p} the power per subcarrier pilot.

By using the prior knowledge that $\mathbf{h}(i)$ has only $\nu+1$ components, an estimate $\tilde{\mathbf{h}}^*(i)$ of the impulse response $\mathbf{h}(i)$ is obtained from the following optimization:

$$\tilde{\mathbf{h}}^*(i) = \min_{\tilde{\mathbf{h}}(i)} \left\| \tilde{\mathbf{H}}(i) - \mathbf{F}\tilde{\mathbf{h}}(i) \right\|^2 \tag{1.14}$$

which yields

$$\tilde{\mathbf{h}}^*(i) = (\mathbf{F}^H\mathbf{F})^{-1}\mathbf{F}^H\tilde{\mathbf{H}}(i) = \mathbf{h}(i) + \mathbf{n}(i) \tag{1.15}$$

where $\mathbf{n}(i) \sim Nc(0, (\mathbf{F}^H\mathbf{F})^{-1}\sigma_e^2)$. This estimate $\tilde{\mathbf{h}}^*(i)$ is feedback to the corresponding transmitter. However, the transmitter receives an impulse response estimate only once every D OFDM symbols, which means that the CSI received at the transmitter will be outdated. The transmitter

uses a minimum-mean-square-error (MMSE) predictor to estimate the actual impulse response. The predicted impulse response $\hat{\mathbf{h}}(i)$ is derived from the P previously received impulse response estimates

$$\mathbf{z}_p(i) \triangleq [\tilde{\mathbf{h}}^*(i-D)^T, ..., \tilde{\mathbf{h}}^*(i-DP)^T]^T.$$

It can be proven that the following relationship holds [46]

$$\mathbf{h}(i) = \hat{\mathbf{h}}(i) + \mathbf{e}(i) \tag{1.16}$$

where $\hat{\mathbf{h}}(i) \sim N_c(\mathbf{0}, \mathbf{R}_h - \mathbf{R}_e)$ and $\mathbf{e}(i) \sim \mathcal{CN}(0, \mathbf{R}_{\mathrm{e}})$. Now, before defining $\mathbf{R}_e$ introducing the matrix $\mathbf{J} \in \mathbb{C}^{P \times P}$ with entries,

$$\mathbf{J}_{k,t} \triangleq \mathrm{J}_0(2\pi f_d D T_s(k-l)) \quad k = 1, ..., P; \quad t = 1, ..., P.$$

Therefore the definition of the channel predictor model can be concluded with

$$\mathbf{R}_{\mathrm{e}} \triangleq \mathbf{R}_h - \mathbf{R}_{\mathbf{h}\boldsymbol{\Psi}_P} \mathbf{R}^{-1}_{\boldsymbol{\Psi}_P \boldsymbol{\Psi}_P} \mathbf{R}^{\mathrm{H}}_{\mathbf{h}\boldsymbol{\Psi}_P}, \tag{1.17}$$

the correlation matrices can be written as follows

$$\mathbf{R}_{\mathbf{h}\boldsymbol{\Psi}_P} = [\mathrm{J}_0(2\pi f_d D T_s), ..., \mathrm{J}_0(2\pi f_d P D T_s)]\, \mathbf{G}\mathbf{R}_c \otimes \mathbf{G}^H$$

$$\mathbf{R}_{\boldsymbol{\Psi}_P \boldsymbol{\Psi}_P} = \mathbf{J} \otimes \mathbf{R}_h + \mathbf{I}_p \otimes (\mathbf{F}^H \mathbf{F})^{-1} \sigma_e^2.$$

The predicted channel gains for the subcarriers are the components of the vector $\hat{\mathbf{H}}(i) = \mathbf{F}\hat{\mathbf{h}}(i)$. The index i will be omitted in the sequel for simplicity. Based on the study performed in [39], we fixed the CSI update interval $D = 7$ and the memory of the predictor $P = 4$ in order to obtain an efficient prediction of the channel and to reduce the signaling over the feedback channel. Also define the average interference from the generic transmitting node l to the qth PU receiver as [39]

$$I_{l,q} \triangleq \mathbf{E}\left\{ \sum_{n=1}^{N} P_{l,n} |H_{l,q,n}|^2 \Big| \left[\widehat{H}_{l,q,m}, m = 1, ..., N \right] \right\} \tag{1.18}$$

$$= \sum_{n=1}^{N} P_{l,n} \mathbf{E} \left\{ |H_{l,q,n}|^2 \middle| \left[\widehat{H}_{l,q,m}, m = 1, ..., N \right] \right\}$$

$$= \sum_{n=1}^{N} P_{l,n} \left(\left| \widehat{H}_{l,q,n} \right|^2 + (\mathbf{V}\mathbf{R}_e\mathbf{V}^H)_{n,n} \right)$$

where, for the last step, we have used the Fourier transform of the eq. (1.16). Further, $H_{l,q,n}$ and $\widehat{H}_{l,q,n}$ represent the actual channel coefficient and the predicted channel coefficient, respectively from ST to the qth PU receiver for $l = 0$, or from the RN R_{i_l} to the qth PU receiver for $1 \leq l \leq L$.

Chapter 2

Goodput Performance Metrics

2.1 Goodput for Multihop

For evaluating the performance of a transmission system we can use many metrics like capacity or outage probability. In this thesis we consider the GP because is able to quantify the trade-off between data rate and link reliability, and it is a more suitable metric to quantify the actual performance of packet-oriented systems, employing practical modulation and coding schemes, respect to the capacity for example. Goodput is defined as the number of information bits delivered in error free packets per unit of time. A generic transmitter of the network is able to optimize the GP by a proper selection of the transmission parameters, if the CSI are perfect. In most wireless networks, because of channel estimation errors and channel feedback delay, this CSI will not be perfect therefore any transmitting node only has CSI and the channel prediction and as a consequence, a PGP, will be optimized. The PGP function is defined as the GP that is achieved when the actual channel is equal to the predicted

channel and depends on the Packet Error Rate (PER). It is well known that PER link performance, of a given coded digital communication over a stationary Additive White Gaussian Noise (AWGN) channel, can be expressed as a function of the Signal To Noise Ratio (SNR). In multi-carrier systems such as Orthogonal Frequency Division Multiplexing (OFDM), however, the frequency selective fading over the transmission channel, introduces large SNR variations across the subcarriers, thus making link PER prediction a demanding task. The need of an accurate yet manageable link level performance figure has led to the Effective SNR Mapping (ESM) concept, where the vector of the received SNRs ($\mathbf{\Gamma}$) across the subcarriers is compressed into a single SNR value, called *effective* SNR and tagged in the sequel as γ_{eff}, that is used to find an estimate of the PER from a basic AWGN link level performance.

In literature, different ESM methods based on different mapping functions have been proposed like Exponential ESM (EESM) based on the pairwise error probability PEP Chernhoff bound for the case of binary signaling. It can be expressed in a simply closed form, but a generalization for high order modulations does not exist. Another solution is the Mutual Information Based ESM (MIESM) that includes two separates models, one for the modulation and the other one for the coding, providing good performance prediction for the mixed-modulation as well. Unfortunately, a closed expression does not exist to calculate the mutual information , so a polynomial approximation is essential. Differently from the conventional ESM methods cited, in this thesis will be use kESM technique. It is represented by the model whose compression function is based on the cumulant moment generating function (CMGF) of the bit level log-likelihood metrics (1.6) at the input of soft decoder [22]. This method offers several significant features compared with other ESM techniques, such as:

- improved accuracy performance compared with the conventional EESM method;
- separation of the modulation and coding models, thus making configurations using mixed modulation among subcarriers easy to manage;
- the use of a tuning factor (required for turbo codes) to offer even improved accuracy that is independent of the modulation format adopted on each subcarrier;
- similar accuracy (or even better for multi-level QAM modulations) as the MIESM method, while offering (unlike the MIESM) a modulation model with a convex and simple closed-form mapping function.

In conclusion we have the following relationship:

$$\mathrm{PER}_{\mathrm{AWGN}}(r, \gamma_{\mathrm{eff}}) \cong \mathrm{PER}_{\mathrm{OFDM}}(\phi, \mathbf{\Gamma}) \tag{2.1}$$

where $\mathbf{\Gamma} = [\gamma_1, \gamma_2, ..., \gamma_N]$ is the set of the instantaneous post-processing SNRs experienced by the subcarriers of a OFDM system (with N the maximum number of subcarriers) and r and ϕ are respectively code rate and modulation. The kESM expression is:

$$\gamma_{\mathrm{eff}} \triangleq -\log\left(\frac{1}{\sum_{j=1}^{N} m_j} \sum_{n=1}^{N} \alpha_n e^{-\hat{\gamma_n}\beta_n}\right), \tag{2.2}$$

where α_n and β_n are constant values depending on the number of coded bits per constellation symbol m_n loaded on the nth subcarrier, and $\hat{\gamma}_n$ is the predicted SNR that is defined as:

$$\hat{\gamma}_n = \frac{P_n \left|\hat{H}_n\right|^2}{\sigma_w^2} \tag{2.3}$$

and $\hat{\mathbf{\Gamma}} = [\hat{\gamma_1}, \hat{\gamma_2}, ..., \hat{\gamma_N}]$ is the predicted SNR vector.

Since the presence of outdated and imperfect CSI at any transmitter, the SNR vector $\mathbf{\Gamma}$ is not known, therefore, the predicted SNR is exploited to evaluate the *effective* SNR (2.2). This method is different from the original formulation of the kESM in [22], where $\mathbf{\Gamma}$ is assumed to be perfectly known by the transmitter but this improvement has been validated in other work [19]. The PGP function can be derived as the ratio of the number normalized by the system bandwidth $\mathrm{B} \triangleq N/T_s$. So we get expressed in (bit/s/Hz), the definition of the PGP function for a single hop as:

$$\begin{aligned} \varsigma(\phi, \mathbf{P}) &\triangleq \frac{T_s}{N} \frac{N_p \left[1 - \mathrm{PER}_{\mathrm{AWGN}}(\mathrm{r}, \gamma_{\mathrm{eff}})\right]}{\frac{N_u T_s}{r \sum_n m_n}} \\ &= \frac{N_p}{N N_u} r \sum_n m_n \left[1 - \mathrm{PER}_{\mathrm{AWGN}}(\mathrm{r}, \gamma_{\mathrm{eff}})\right] \end{aligned} \tag{2.4}$$

This is the result for a generic single link. For find the PGP in a multi hop network first of all we consider a generic path $\mathcal{P}(\mathrm{ST}, \mathrm{R}_{i_1}, \cdots, \mathrm{R}_{i_L}, \mathrm{SR})$ through $L \leq M$ relay. The probability of a packet error from ST to SR is defined as

$$\begin{aligned} \mathrm{PER}^{\mathrm{total}}_{\mathrm{AWGN}}(\mathrm{r}_0, ..., \mathrm{r}_\mathrm{L}, \gamma_{0,\mathrm{eff}}, ..., \gamma_{\mathrm{L,eff}}) &\triangleq \mathrm{PER}_{\mathrm{AWGN}}(\mathrm{r}_0, \gamma_{\mathrm{eff}}) \\ &+ \left[1 - \mathrm{PER}_{\mathrm{AWGN}}(\mathrm{r}_0, \gamma_{0,\mathrm{eff}})\right] \cdot \mathrm{PER}_{\mathrm{AWGN}}(\mathrm{r}_1, \gamma_{1,\mathrm{eff}}) \\ ... + \prod_{i=1}^{L-1} \left[1 - \mathrm{PER}_{\mathrm{AWGN}}(\mathrm{r}_i, \gamma_{i,\mathrm{eff}})\right] &\cdot \mathrm{PER}_{\mathrm{AWGN}}(\mathrm{r}_\mathrm{L}, \gamma_{\mathrm{L,eff}}) \end{aligned} \tag{2.5}$$

From (2.5), the normalized PGP (bits/s/Hz) of the L DF RNs is written as follows

$$\begin{aligned} \varsigma(\phi_0, ..., \phi_L, \mathbf{P}_0, ..., \mathbf{P}_L) &\triangleq \frac{T_s}{N} \frac{N_p \left[1 - \mathrm{PER}^{\mathrm{total}}_{\mathrm{AWGN}}(\mathrm{r}_0, ..., \mathrm{r}_\mathrm{L}, \gamma_{0,\mathrm{eff}}, ..., \gamma_{\mathrm{L,eff}})\right]}{\sum_{j=0}^{L} \frac{N_u T_s}{r_j \sum_n m_{j,n}}} \\ &= \frac{N_p}{N N_u} \frac{\left[1 - \mathrm{PER}^{\mathrm{total}}_{\mathrm{AWGN}}(\mathrm{r}_0, ..., \mathrm{r}_\mathrm{L}, \gamma_{0,\mathrm{eff}}, ..., \gamma_{\mathrm{L,eff}})\right]}{\sum_{j=0}^{L} \frac{1}{r_j \sum_n m_{j,n}}} \end{aligned} \tag{2.6}$$

where $\phi_0 = \{\mathbf{m}_0, \mathrm{r}_0\}$, $\phi_l = \{\mathbf{m}_l, \mathrm{r}_l\}$, $\mathbf{P}_0$ and $\mathbf{P}_l$ respectively denote the TM for the ST and RN R_{i_l} and the transmit power per symbol for the ST and RN R_{i_l}. The denominator $\sum_{j=0}^{L} \frac{1}{r_j \sum_n m_{j,n}}$ in (2.6) represents the total transmission time of a packet from ST to SR through L RNs. The transmission time of a packet for each link can vary, because it depends on the code-rate $r_{l,j}$ and the number of bits per subcarrier $m_{l,j,n}$ that may be different from a link to another.

2.2 Approximated Goodput

For reduce the signaling traffic between relay nodes and ST and for reduce the computational complexity an approximation of the PGP is proposed. Thanks to this approximation we will define a more efficient path selection strategy between ST and SR that will be presented later. The Approximated PGP (A-PGP) function is defined as:

$$\tilde{\varsigma}(\phi_0, ..., \phi_L, \mathbf{P}_0, ..., \mathbf{P}_L) \triangleq \frac{N_p}{N N_u} \frac{\left[1 - \widetilde{\mathrm{PER}}^{\,\mathrm{total}}_{\mathrm{AWGN}}(\mathrm{r}_0, ..., \mathrm{r}_\mathrm{L}, \gamma_{0,\mathrm{eff}}, ..., \gamma_{\mathrm{L,eff}})\right]}{\sum_{j=0}^{L} \frac{1}{r_j \sum_n m_{j,n}}} \tag{2.7}$$

where

$$\widetilde{\mathrm{PER}}^{\,\mathrm{total}}_{\mathrm{AWGN}}(\mathrm{r}_0, ..., \mathrm{r}_\mathrm{L}, \gamma_{0,\mathrm{eff}}, ..., \gamma_{\mathrm{L,eff}}) \triangleq \sum_{i=0}^{L} \mathrm{PER}_{\mathrm{AWGN}}(\mathrm{r}_i, \gamma_{i,\mathrm{eff}}) \tag{2.8}$$

The probability (2.7) considers the loss of a packet as an independent event on each link between ST and SR. The approximation (2.7) of the true probability (2.5) is based on the fact that $\mathrm{PER}_{\mathrm{AWGN}}(\mathrm{r}_l, \gamma_{l,\mathrm{eff}}) << 1$ and consequently $(1 - \mathrm{PER}_{\mathrm{AWGN}}(\mathrm{r}_l, \gamma_{l,\mathrm{eff}})) \approx 1)$ for high values of *effective* SNR $\forall l \in \mathcal{L}$. The use of the A-PGP causes only a negligible reduction of the GP performance, respect to the PGP function (Figure 5.5). This is will be shown in Chapter 5. In Figure (2.1) we can see

the trend of the PER function for different code rates and values of γ_{eff}. Considering a PER value of 0.1 we get the values of γ_{eff} shown in the Table 2.1 below the figures. So we can know the values of transmission power, Figure (2.2), for which the condition $\text{PER}_{\text{AWGN}}(\text{r}_l, \gamma_{l,\text{eff}}) << 1$ is satisfied and therefore the probability (2.7).

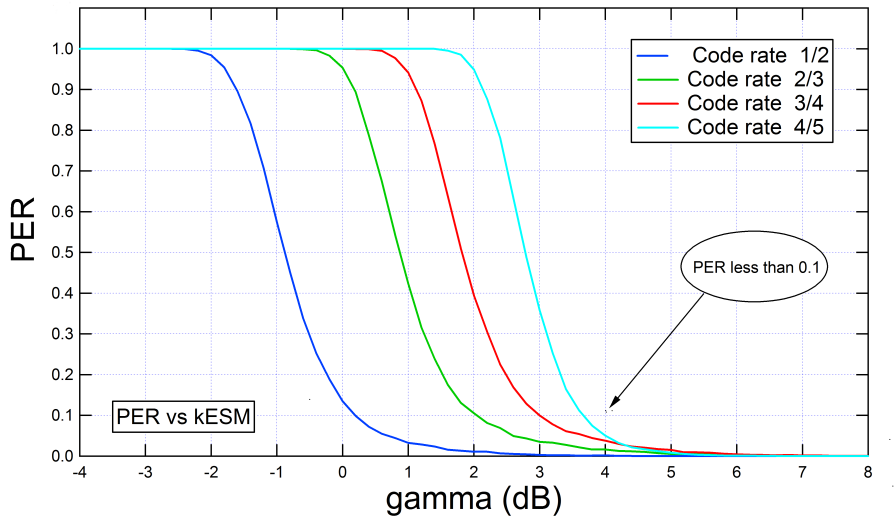

Figure 2.1: PER vs Effective SNR

Code rate	$\gamma_{\text{eff}}(dBm)$
1/2	0.2
2/3	2.2
3/4	3.0
4/5	3.6

Table 2.1: Corresponding values of γ_{eff} for PER ≤ 0.1

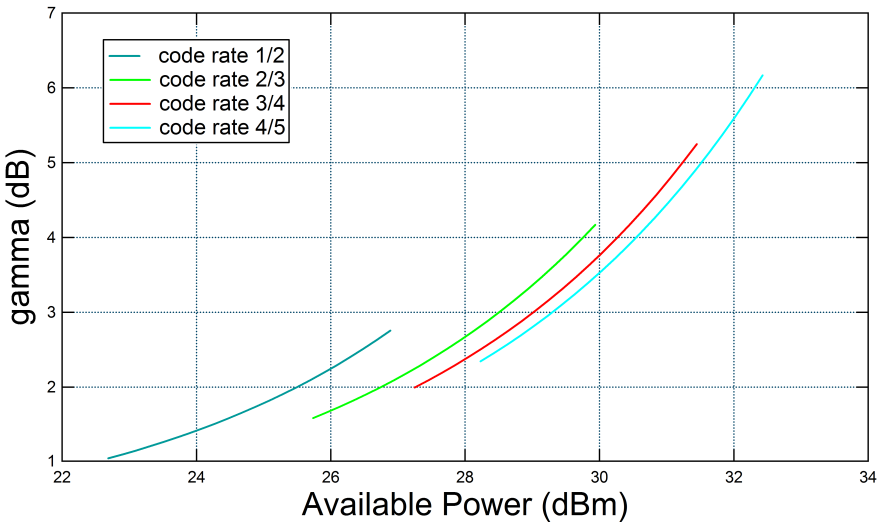

Figure 2.2: Effective SNR vs Available Power

Chapter 3

Resource Allocation

3.1 Resource Allocation problem

Now focus our attention on the problem of how to allocate the available radio resource appropriately so that we can get the best link performance for any given channel conditions. Efficient RA in non cooperative cognitive radio network is essential in order to meet the challenges of future wireless networks. Knowledge of channel state information is a signicant input parameter. Here resource allocation algorithms assume that CSI is known at both transmitter and receiver but is outdated. Our RA techniques are able to select the transmission mode (TM) and power vector ($\mathbf{P}$) for a packed-oriented BIC-OFDM system in order to maximize the objective function, so that a robust and spectrally-efficient transmission over frequency selective channels is obtained. In this section two different RA algorithms are presented for the system model illustrate in Chapter 1: *optimal* and *local* resource allocation. The difference between this two approaches is in the respective objective function. In the Optimal-RA (O-RA) the objective function is the end-to-end PGP (2.6). Due to its complexity and to a high signaling traffic, O-RA is used only as bench-

mark, and it is derived from [19], where the RA algorithm is shown for dual-hop transmissions. Instead in the new and much simpler Local-RA (L-RA) problem objective function is the A-PGP (2.8). Thanks to this approach, L-RA method requires a considerably lower feedback information from each RN and the SR to the ST respect to the O-RA method. Before explaining in detail the different methods, let us fix a generic path $\mathcal{P}(\mathrm{ST}, \mathrm{R}_{i_1}, \cdots, \mathrm{R}_{i_L}, \mathrm{SR})$ through L of the M available RNs for each presented RA technique. Furthermore, let us define the optimal TM and power allocation vector that are the transmission parameters for the generic link $l \in \mathcal{L}$ as

$$\begin{aligned} \phi_l^* &\triangleq \{\mathbf{m}_l^*, \mathrm{r}_\mathrm{l}^*\} \\ \mathbf{P}_l^* &\triangleq \left[\mathrm{P}_{l,1}^*, ..., \mathrm{P}_{l,N}^*\right]^T \end{aligned} \tag{3.1}$$

where $\mathbf{m}_l^* = \left[\mathrm{m}_{l,1}^*, ..., \mathrm{m}_{l,N}^*\right]^T$, r_l^* and $\mathrm{P}_{l,n}^*$ are respectively the number of loaded bits per subcarrier, the selected code rate and the allocated power over the subcarrier n. From here, moreover, uniform bit allocation (UBA), $m_{l,n} = m_l$, $\forall n \in \mathcal{N}$, $\forall l \in \mathcal{L}$, is adopted for simplicity.

3.2 Optimal Resource Allocation Solutionn

O-RA consists in optimizing the PGP object function between ST and SR, in the domain of the power allocation (PA) and the TM subject the constraints on the transmitted power and the finite set Φ of allowable TMs. Mathematically the RA optimization problem (OP) can be introduced as:

$$(\phi_0^*, ..., \phi_L^*, \mathbf{P}_0^*, ..., \mathbf{P}_L^*) = \arg \max_{\phi_0,...,\phi_L,\mathbf{P}_0,...,\mathbf{P}_L} \{\zeta(\phi_0, ..., \phi_L, \mathbf{P}_0, ..., \mathbf{P}_L)\} \tag{3.2}$$

$$\sum_{n=1}^{N} P_{l,n} \leq P_{tot} \quad \forall l \in \mathcal{L}$$

$$P_{l,n} \geq 0 \quad \forall n \in \mathcal{N}, \quad \forall l \in \mathcal{L}$$

$$I_{l,q} \leq \mathcal{I}_q, \quad \forall q \in \mathcal{Q}, \quad \forall l \in \mathcal{L}$$

Problem (3.2) is a mixed integer OP, which includes both variables belonging to a discrete finite-size set ϕ_l and continuous-valued variables ($\mathbf{P}_l$). Moreover, given the specific structure of the objective function, the OP can be solved into two consecutive steps:

1. given a generic TM ϕ_l , find the optimal PA vector $\mathbf{P}_l^*$
2. the best TM ϕ_l^* is selected in order to maximize the PGP metric.

As regards the first point, if we keep the global goodput expression (2.5) we can see that the PGP depends on the power allocation vector $\mathbf{P}_l$ only through the effective SNR $\gamma_{l,\text{eff}}(\phi_l, \mathbf{P}_l)$. Furthermore, since the $\text{PER}_{\text{AWGN}}^{\text{total}}$ decreases when the $\gamma_{l,\text{eff}}(\phi_l, \mathbf{P}_l)$ increases, then the optimal power allocation vector $\mathbf{P}_l$ can be found for a given value of ϕ_l by maximizing $\gamma_{l,\text{eff}}(\phi_l, \mathbf{P}_l)$. For this reasons we can introduce the following independent OP $\forall l \in \mathcal{L}$:

$$\mathbf{P}_l^* = \arg\max_{\mathbf{P}_l} \{\gamma_{l,\text{eff}}(\phi_l, \mathbf{P}_l)\} \tag{3.3}$$

$$= \arg\min_{\mathbf{P}_l} \{\chi_l(\mathbf{m}_l, \mathbf{P}_l)\} \tag{3.4}$$

$$\sum_{n=1}^{N} P_{l,n} \leq \mathrm{P}_{tot}$$

$$P_{l,n} \geq 0 \quad \forall n \in \mathcal{N},$$

$$I_{l,q} \leq \mathcal{I}_q, \quad \forall q \in \mathcal{Q} \tag{3.5}$$

with the new objective function

$$\chi_l(\mathbf{m}_l, \mathbf{P}_l) \triangleq \sum_{n=1}^{N} \alpha_{l,n} \cdot e^{-\hat{\gamma}_{l,n}\beta_{l,n}} \tag{3.6}$$

It is easy to see that the OP remains unchanged, replacing the objective function (3.3) by (3.4), because a generic TM ϕ_l is fixed. The considered OP (3.4) is a convex optimization problem [43], and the optimal solution can be found by the method of Lagrange multipliers. However, the convergence of such algorithms is often slow. Therefore we will use the Successive Set Reduction (SSR) approach introduced in [44]. In [44], the SSR algorithm is shown to achieve almost the same performance as the method of Lagrange multipliers but with a much faster convergence. We also note that the optimal value of $\mathbf{P}_l$ only depends on the modulation vector $\mathbf{m}_l$ and $\hat{\mathbf{H}}_l$.

In the second step we obtain the optimal TM ϕ^* by solving the following problem:

$$(\phi_0^*, ..., \phi_L^*) = \arg \max_{\phi_0,...,\phi_L} \{\zeta(\phi_0, ..., \phi_L, \mathbf{P}_0, ..., \mathbf{P}_L)\} \tag{3.7}$$

$$\phi_l \in \mathcal{D}_m^N \times \mathcal{D}_r, \quad \forall l \in \mathcal{L}$$

$$m_{l,n} = m_l, \quad \forall n \in \mathcal{N}, \quad \forall l \in \mathcal{L}$$

OP (3.7) is optimally solved by means of an exhaustive search, because the variables ϕ_l belong to a discrete finite-size set. Pseudo-code of the O-RA problem is shows in Tab.3.1. At this point the limitation of the O-RA algorithm for a multi-hop scenario is explained better because must know:

- predicted SNR vector $\hat{\mathbf{\Gamma}}_l$ (with $\mathbf{P}_{l,n} = 1, \forall l \in \mathcal{L}, \forall n \in \mathcal{N}$) of each link belonging to a given path when evaluating the objective function (3.6);

- predicted channel vectors $\hat{\mathbf{H}}_{l,q}$ from any node of a given path towards the PUs when evaluating the interference constraints (3.5).

These requirements may lead to a high signaling traffic, causing a congestion of the feedback channel towards the ST. Moreover, OP (3.7) is solved in an exhaustive way and this causes an exponential growth in computational complexity, directly proportional to the number of the RNs. Therefore, the O-RA is a complex centralized method and it does not seem interesting in a multi-hop conguration, where it is of paramount importance to keep low the CSI over the feedback channel. However, O-RA algorithm returns an optimal solution and consequently it will be used to provide a benchmark to the L-RA that will be presented in the next section.

3.3 Local Resource Allocation Solution

The optimal energy allocation (3.3) and the optimal TM (3.7) solution are found in order to maximize the PGP from the ST to the SR but as mentioned above, this approach is not very efficient. Local-RA strategy (L-RA) is presented with the aim to tackle the problems that arises exploiting the O-RA method. L-RA can effectively reduce the computational complexity to the ST and the signaling over the feedback channel because essentially maximizes the PGP (2.4) for each transmitting node. That is the (2.4) is now the object function and every node can allocate $\mathbf{P}_l$ and ϕ_l with the other node directly connected to it. The RA OP for the generic link $l \in \mathcal{L}$ is:

$$(\phi_L^*, \mathbf{P}_L^*) = \arg \max_{\phi_L, \mathbf{P}_L} \{\zeta (\phi_L, \mathbf{P}_L)\} \tag{3.8}$$

$$\sum_{n=1}^{N} P_{l,n} \leq \mathrm{P}_{tot},$$

$$P_{l,n} \geq 0 \quad \forall n \in \mathcal{N},$$

$$I_{l,q} \leq \mathcal{I}_q, \quad \forall q \in \mathcal{Q},$$

It follows that, OP (3.8) is solved in two steps, as for the O-RA OP. The D-RA problem, therefore, is divided into two consecutive steps:

1. given a generic TM ϕ_l , find the optimal power allocation vector $\mathbf{P}_l^*$
2. the best TM ϕ_l^* is selected in order to maximize the PGP metric (2.4)

For first step, the optimal power allocation vector $\mathbf{P}_l$ is calculated from the OP (3.3) while the optimal TM ϕ_l, in second step, is obtained by exhaustively solving the following problem

$$\begin{aligned} \phi_L^* &= \arg\max_{\phi_L} \{\zeta(\phi_L, \mathbf{P}_L)\} \\ \phi_l &\in \mathcal{D}_m^N \times \mathcal{D}_r \\ m_{l,n} &= m_l, \quad \forall n \in \mathcal{N} \end{aligned} \tag{3.9}$$

Obviously, the L-RA method is sub-optimal compared with the O-RA. In detail, exploiting the L-RA strategy, the local GP between two generic nodes is maximized, without taking into consideration the end to end GP from ST to SR. In other words, the packet transmission time from ST to SR is not considered and this makes up to a big problem that can be solved by the path selection strategy presented in the next chapter. However, carrying out the local maximization of the GP, the ST has no need to know the CSI of each link as in the O-RA strategy therefore, the wireless network obtains a significant reduction of the signaling over the feedback channel. This is the big difference between O-RA and L-RA. Tab.3.2 shows the pseudo-code of the L-RA algorithm.

Given a generic path $\mathcal{P}(\mathrm{ST}, \mathrm{R}_{i_1}, \cdots, \mathrm{R}_{i_L}, \mathrm{SR})$;

Initialize: $\bar{m}_0 = 0, \ldots, \bar{m}_L = 0$, $\mathbf{r} = [1/2, 2/3, 3/4, 5/6]^{\mathrm{T}}$, $\zeta_{\mathrm{temp}} = 0$;

For $\bar{m}_0 = 2 : 2 : m_{0,\max}$;

.
.
.

For $\bar{m}_L = 2 : 2 : m_{L,\max}$;

$\forall l \in \mathcal{L}$, **Evaluate** $\bar{\mathbf{P}}_l$ according the OP (3.4);

For $i_0 = 1 : \mathrm{length}(\mathbf{r})$;

$\bar{r}_0 = \mathbf{r}(i_0)$;

.
.
.

For $i_L = 1 : \mathrm{length}(\mathbf{r})$;

$\bar{r}_L = \mathbf{r}(i_L)$;

Compute:

$\forall l \in \mathcal{L}$, $\gamma_{l,\mathrm{eff}}(\bar{\phi}_l, \bar{\mathbf{P}}_l)$ in (2.2);

$\zeta(\bar{\phi}_0, \cdots \bar{\phi}_L, \bar{\mathbf{P}}_0, \cdots, \bar{\mathbf{P}}_L)$ in (2.6);

If $\zeta(\bar{\phi}_0, \cdots \bar{\phi}_L, \bar{\mathbf{P}}_0, \cdots, \bar{\mathbf{P}}_L) \geq \zeta_{\mathrm{temp}}$

Then $\forall l \in \mathcal{L}$

Set $\phi_l^* = \{\bar{m}_l, \bar{r}_l\}$, $\mathbf{P}_l^* = \bar{\mathbf{P}}_l$, $\zeta_{\mathrm{temp}} = \zeta(\bar{\phi}_0, \cdots, \bar{\phi}_L, \bar{\mathbf{P}}_0, \cdots, \bar{\mathbf{P}}_L)$;

End If

End For

.
.
.

End For

End For

.
.
.

End For

Return $\forall l \in \mathcal{L}$, ϕ_l^* and $\mathbf{P}_l^*$

Table 3.1: **O-RA pseudo-code**

Given a generic path $\mathcal{P}(\mathrm{ST}, \mathrm{R}_{i_1}, \cdots, \mathrm{R}_{i_L}, \mathrm{SR})$;

Initialize: $\bar{m}_l = 0$, $\mathbf{r} = [1/2, 2/3, 3/4, 5/6]^{\mathrm{T}}$, $\zeta_{\mathrm{temp}} = 0$;

For $\bar{m}_l = 2 : 2 : m_{l,\max}$;

Evaluate $\bar{\mathbf{P}}_l$ according the OP (3.4);

For $i_l = 1 : \mathrm{length}(\mathbf{r})$;

$\bar{r}_l = \mathbf{r}(i_l)$;

Compute:

$\gamma_{l,\mathrm{eff}}(\bar{\phi}_l, \bar{\mathbf{P}}_l)$ in (2.2);

$\zeta(\bar{\phi}_l, \bar{\mathbf{P}}_l)$ in (2.4);

If $\zeta(\bar{\phi}_l, \bar{\mathbf{P}}_l) \geq \zeta_{\mathrm{temp}}$

Then

Set $\phi_l^* = \{\bar{m}_l, \bar{r}_l\}$, $\mathbf{P}_l^* = \bar{\mathbf{P}}_l$, $\zeta_{\mathrm{temp}} = \zeta(\bar{\phi}_l, \bar{\mathbf{P}}_l)$;

End If

End For

End For

Return ϕ_l^* and $\mathbf{P}_l^*$

Table 3.2: **L-RA pseudo-code**

Chapter 4

Path Selection

4.1 Optimal Path Selection

In this chapter we tackle the problem of finding a suitable path between source (ST) and destination (SR) in the multi hop network. In other words, from a set of M available RNs in the network, a path $\mathcal{P}$ with $L \leq M$ relays, will be selected to provide the "best" GP between ST and SR. We present three different PS approaches, which are called Optimal PS (O-PS), Sub-Optimal PS (Sub-PS) and Approximated Sub-PS (ASub-PS) respectively. The first method, O-PS, will be not really used if no as a benchmark for the second and third ones, because the signaling traffic over the feedback channel and complexity are unsustainable when increasing the number of relay. It must be underlined that we modified the PS methods presented in [18], in order to obtain the Sub-PS and ASub-PS strategies for a packet-oriented BIC-OFDM modulation, including also the GP metric to evaluate the performance of the transmission. O-PS method can be nalized by selecting the path that maximizes the overall PGP metric from the ST to the SR. The PS problem can be formulated as:

$$\mathcal{P}_{\text{opt}} \triangleq \arg\max_{\mathcal{P}\in\mathcal{G}} \{\eta(\mathcal{P})\} \tag{4.1}$$

where $\mathcal{G}$ is the set of all possible paths connecting ST with SR and the objective function is

$$\eta(\mathcal{P}) \triangleq \zeta(\phi_0^*, ..., \phi_L^*, \mathbf{P}_0^*, ..., \mathbf{P}_L^*) \tag{4.2}$$

The optimal path $\mathcal{P}_{\text{opt}}$ is found in an exhaustive way. In detail, the problem (4.7) is solved in two steps:

- O-RA method is performed for any path belonging to the set $\mathcal{G}$
- the best PGP $\zeta(\phi_0^*, ..., \phi_L^*, \mathbf{P}_0^*, ..., \mathbf{P}_L^*) \in \mathcal{G}$ therefore the best path $\mathcal{L} \in \mathcal{G}$ is found

In a network with M RNs exist $M!/(M-L)!$ different routes to connect ST to SR passing through $L \leq M$ RNs. As a consequence, problem (4.7) was solved with an exhaustive search requires combinatorial complexity, which even for small M is clearly unfeasible. Moreover, in order to solve the O-PS problem (4.7), ST needs to know the CSI $\mathbf{\Gamma}_l$ of all active RNs. In this way, the signaling trafc over the feedback channel will be unsustainable. Subsequently, ST should transmit the best TM ϕ_l^* and the best power allocation $\mathbf{P}_l^*$ to every RN R_{i_l}, $\forall l \in \mathcal{L}$. Thus, O-PS method is considered only as a benchmark for the methods here proposed. The pseudo code for O-PS is show in Table 4.1.

4.2 Sub-optimal Path Selection

The Sub-PS method provides a much more efficient path selection algorithm, whose rationale relies on:

($K_{\mathcal{G}}$ is the total number of path $\mathcal{P} \in \mathcal{G}$)
Initialize: $\eta(\mathcal{P}_k) = 0$;
For $k = 1 : K_{\mathcal{G}}$;
  Evaluate $\bar{\eta}(\mathcal{P}_k)$ according to the O-RA (3.2);
  If $\bar{\eta}(\mathcal{P}_k) \geq \eta(\mathcal{P}_k)$ **Then**
  Set $\mathcal{P}_{\text{opt}} = \mathcal{P}_k$;
  End If
End For
Return $\mathcal{P}_{\text{opt}}$

Table 4.1: **O-PS pseudo-code**

- first finding the set of candidates, i.e., one path for each value of L, with $0 \leq L \leq M$
- to define a cost metric for each link of the network
- then, choosing the best path in the candidate set as the one which maximizes the A-PGP metric (2.7)

We use the A-PGP metric to solve the Sub-PS problem. Indeed, by means of the approximation of the PGP, we can exploit a sum of PER that is very useful to approximately find the shortest path. It is necessary to define a cost metric for each link of the network and this cost is the PER defined in (2.1). Each transmitting node performs first the RA method, in order to nd the optimal TM ϕ_l and power allocation vector $\mathbf{P}_l^*$ (3.1), and then each one evaluates the PER (2.1). In detail, to execute the Sub-PS method, two steps are needed:

1. the network performs the L-RA algorithm

2. each transmitting node $\mathrm{R}_{\mathrm{i}_l}$ evaluates the cost as

$$\delta_{\mathrm{R}_{\mathrm{i}_l}-\mathrm{R}_{\mathrm{i}_{l+1}}} \triangleq \mathrm{PER}_{\mathrm{AWGN}}(\mathrm{r}_l^*, \gamma_{l,\mathrm{eff}}^*) \tag{4.3}$$

where $\mathrm{R}_{\mathrm{i}_{l+1}}$ represents each node directly connected to $\mathrm{R}_{\mathrm{i}_l}$. For $l = 0$ the cost is $\delta_{\mathrm{ST}-\mathrm{R}_{\mathrm{i}_1}}$ and for $l = L$ the cost is $\delta_{\mathrm{R}_{\mathrm{i}_l}-\mathrm{SR}}$.

At this point the solution for the Sub-PS problem can be obtained with polynomial complexity $\mathcal{O}(M^3)$ by means of a two-step procedure:

Step 1) The $M+1$ sub-problems

$$\mathcal{P}_{\mathrm{Sub-PS}}^{(L)} = \underset{\mathcal{P}\in\mathcal{G}_L}{\arg\min}\,\{\mu(\mathcal{P})\} \qquad 0 \le L \le M \tag{4.4}$$

are solved adopting the path metric

$$\mu(\mathcal{P}) \triangleq \sum_{l=0}^{L} \delta_{R_{i_l}-R_{i_{l+1}}} = \sum_{i=0}^{L} \mathrm{PER}_{\mathrm{AWGN}}(\mathrm{r}_i^*, \gamma_{i,\mathrm{eff}}^*) \tag{4.5}$$

$$= \widetilde{\mathrm{PER}}_{\mathrm{AWGN}}^{\mathrm{total}}(\mathrm{r}^*0, ..., \mathrm{r}_{\mathrm{L}}^*, \gamma_{0,\mathrm{eff}}^*, \cdots, \gamma_{\mathrm{L,eff}}^*) \tag{4.6}$$

where $\mathcal{G}_L \triangleq \{\mathcal{P}|\mathcal{P} \in \mathcal{G}$ and passes through L RNs only$\}$. The result is the set $\mathcal{C} \triangleq \left\{\mathcal{P}_{\mathrm{Sub-PS}}^{(L)}\right\}_{L=0}^{M}$, which includes the $M+1$ candidates for the optimal path.

Step 2) The final selected path follows from

$$\mathcal{P}_{\mathrm{Sub-PS}} = \underset{\mathcal{P}\in\mathcal{C}}{\arg\max}\,\{\widetilde{\eta}(\mathcal{P})\} \tag{4.7}$$

with the objective function defined as

$$\widetilde{\eta}(\mathcal{P}) \triangleq \widetilde{\zeta}(\phi_0^*, ..., \phi_L^*, \mathbf{P}_0^*, ..., \mathbf{P}_L^*) \tag{4.8}$$

and $\widetilde{\zeta}(\phi_0^*, ..., \phi_L^*, \mathbf{P}_0^*, ..., \mathbf{P}_L^*)$ is the A-PGP metric (2.7).

Therefore summing up what was said, with Sub-PS algorithm we have all the paths belonging to $\mathcal{G}_L$ have L relays. A-PGP function $\widetilde{\eta}(\mathcal{P})$ increases with decreasing the function $\mathrm{PER}_{\mathrm{AWGN}}^{\mathrm{total}}$ (2.8), then maximizing $\widetilde{\zeta}$ is equivalent to minimize $\mu(\mathcal{P})$ (4.5) only if optimal TM ϕ_l^* and power vector $\mathbf{P}_l^*$ are calculated before for any link of the network, i.e., by means of the D-RA algorithm. Moreover, $\mu(\mathcal{P})$ is an additive metric, i.e., it is the sum of the positive weights $\delta_{\mathrm{R}_{\mathrm{i}_l}-\mathrm{R}_{\mathrm{i}_{l+1}}}$ belonging to the path P. Hence, each sub-problem (4.4) of Step 1 turns into a shortest path problem constrained by L hops with non-negative link metric $\delta_{\mathrm{R}_{\mathrm{i}_l}-\mathrm{R}_{\mathrm{i}_{l+1}}}$, which can be efficiently solved with polynomial complexity by applying the modified Bellman-Ford (BF) algorithm [45]. Pseudo code is show in Table 4.2. The approximation of the PGP with the A-PGP, therefore, is necessary to validate the previous proposition. In this case, ST requires only ϕ_l^* and $\delta_{\mathrm{R}_{\mathrm{i}_l}-\mathrm{R}_{\mathrm{i}_{l+1}}}$ $\forall l \in \mathcal{L}$, as information to perform the Sub-PS algorithm and subsequently ST sends a signal in the network to activate the chosen RNs. It should therefore be emphasised that the signaling over the feedback channel is drastically reduced compared to O-PS solution.

4.3 Approximated Sub-optimal Path Selection

Another approximation can be introduced for to reduce the overall computational complexity of the Sub-PS algorithm. The approximated version of the Sub-PS algorithm, or ASub-PS for short, can be defined by the following OP:

$$\mathcal{P}_{\mathrm{ASub-PS}}^{(\mathrm{opt})} \triangleq \underset{\mathcal{P}\in\mathcal{G}}{\arg\min} \left\{\mu(\mathcal{P})\right\}, \tag{4.9}$$

(J is the total number of links)

For $j = 1 : J$;

Evaluate ϕ_j^*, $\mathbf{P}_j^*$ according to the L-RA (3.9)

and $\delta_{\mathrm{R}_{i_j}-\mathrm{R}_{i_{j+1}}} = \Phi_{\mathrm{AWGN}}(r_j^*, \gamma_{j,\mathrm{eff}}^*)$ (4.3);

End For

For $L = 0 : M$;

Select $\mathcal{P}_{\mathrm{Sub-PS}}^{(L)} = \underset{\mathcal{P}\in\mathcal{G}_L}{\mathrm{argmin}}\{\mu(\mathcal{P})\}$ (4.4);

Set $\mathcal{C}(L) = \mathcal{P}_{\mathrm{Sub-PS}}^{(L)}$;

End For

Select $\mathcal{P}_{\mathrm{Sub-PS}}^{(\mathrm{opt})} = \underset{\mathcal{P}\in\mathcal{C}}{\mathrm{argmax}}\{\widetilde{\eta}(\mathcal{P})\}$ (4.7);

Return $\mathcal{P}_{\mathrm{Sub-PS}}^{(\mathrm{opt})}$

Table 4.2: **Sub-PS pseudo-code**

where $\mu(\mathcal{P})$ is dened in (4.5). Basically, ASub-PS algorithm does not consider the transmission time of a packet from ST to SR, differently from the Sub-PS method and because the metric $\mu(\mathcal{P})$ is additive on the links belonging to a given path $\mathcal{P}$, this problem is equivalent to an unconstrained shortest path problem with non-negative link costs, which can be efficiently solved through the Fibonacci-heap-based Dijkstra algorithm with complexity $\mathcal{O}(M^2)$. So the OP (4.9) can be solved in $\mathcal{O}(M^2)$ compared to $\mathcal{O}(M^3)$ for Sub-PS algorithm. However, ASub-PS represents a good performance-versus-complexity tradeoff as we will show in the numerical results and its pseudo code is show in Table 4.3. Moreover, the signaling over the feedback channel is further reduced, respect to O-PS and Sub-PS. ST, indeed, only needs $\delta_{\mathrm{R}_{i_l}-\mathrm{R}_{i_{l+1}}}$, $\forall l \in \mathcal{L}$ to perform the ASub-PS algorithm.

(J is the total number of links)

For $j = 1 : J$;

Evaluate ϕ_j^*, $\mathbf{P}_j^*$ according to the L-RA (3.9)

and $\delta_{\mathrm{R}_{i_j}-\mathrm{R}_{i_{j+1}}} = \Phi_{\mathrm{AWGN}}(r_j^*, \gamma_{j,\mathrm{eff}}^*)$ (4.3);

End For

Select $\mathcal{P}_{\mathrm{ASub-PS}}^{(\mathrm{opt})} = \underset{\mathcal{P}\in\mathcal{G}}{\operatorname{argmin}} \{\mu(\mathcal{P})\}$ (4.9);

Return $\mathcal{P}_{\mathrm{ASub-PS}}^{(\mathrm{opt})}$

Table 4.3: **ASub-PS pseudo-code**

Chapter 5

Simulation

In this section, we evaluate the performance, in terms of GP, of the L-RA combined with Sub-PA and ASub-PS, by comparing them with the optimal benchmark O-RA and O-PS. For this purpose have been considered four different network configurations (NCs) or scenarios as depicted in Figure 5.1, 5.2, 5.3, 4. The RNs are fixed in all NC except for NC4. In each simulation the number of PU receivers is $N_{PU} = 1$ in the same bandwidth B of the multi-hop system and it is randomly positioned along the green line, except for the conguration NC4, where it is randomly positioned within the green square. Convolutional code have been used to simplify the processing during the soft-demodulation, however, we also could consider turbo code. The parameters of the CR BIC-OFDM system and of the channel predictor are summarized in Tabella 5.1 VI. ITU vehicular A channel [47] and modied Cost231 Hata [48] models are exploited. GP value is calculated by averaging the number of bits/s/Hz correctly received on $N_{pkt} = 1000$ transmitted packet over independent channel realizations. The *average* GP (AGP), therefore, is defined as:

$$\varsigma_{avg} \triangleq \frac{1}{N_{pkt}} \frac{1}{B} \sum_{k=1}^{N_{pkt}} \frac{N_p \delta(k)}{T_{pkt}(k)} \tag{5.1}$$

where $\delta(k) = 1$ if the kth packet was correctly received, otherwise 0 and $T_{pkt} = T_s \cdot N_{OFDM}(k)$ is the transmission time of the packet k. The simulations have been made varying the available power P_{tot} that is equal for all nodes of the network. This is because, all nodes, including PU, can be positioned at different distances each other, therefore, the path loss changes and the received SNR is different among the nodes for equal transmitted power.

First of all, we evaluate the different between PGP and A-PGP or more precisely, verify the accuracy of the A-PGP function (2.7). The scenario is show in Figure 5.3 and consist of two fixed relays in square configuration while PU is randomly positioned along the dashed line. The PGP and A-PGP values are obtained solving the O-RA problem and the O-PS one. As we can see, the two curves are practically identical. A small gap is visible for $P_{\text{tot}} \leq 14$ dBm, because the A-PGP is based on the fact that $\text{PER}_{\text{AWGN}}(\text{r}_l, \gamma_{l,\text{eff}}) << 1$, $\forall l \in L$, and consequently, in the case of low transmitted power, the values of $\text{PER}_{\text{AWGN}}(\text{r}_l, \gamma_{l,\text{eff}})$ increase, $\forall l \in L$. For these reasons, as mentioned in Section 2.2, we have fixed a low PER value (Figure 2.1) and determinate the corresponding γ for PER function with different code rate. Then we have obtained the transmission power range of P_{tot} as show in Figure 2.2. In the considered range from 16 to 34 dBm, the A-PGP is confirmed to be an excellent approximation of the PGP function and, therefore, the A-PGP can be used to solve the Sub-PS problem.

The performance of the L-RA method is evaluated, considering the scenarios NC1 and NC2, where the path is fixed. The Figures 5.6 and 5.7 confirm that the L-RA is a good sub-optimal method to solve the RA problem compared with the O-RA. Indeed, there is not an appreciable loss of AGP performance. Therefore, L-RA solution can be exploited to allocate the resource in the network, to reduce the signaling among

the nodes and to calculate the costs of the link $\delta_{\mathrm{R}_{i_l}-\mathrm{R}_{i_{l+1}}}$, $\forall l \in \mathcal{L}$ which are necessary in the Sub-PS algorithm and ASub-PS one. Moreover, observing the performance in Fig. 5.7 we note that the AGP is always lower than that in Fig. 5.6, because in NC2 is present one RN in more and the transmission time of a packet from ST to SR inevitably increases.

Now, we can demonstrate the effectiveness of the L-RA combined with Sub-PA and ASub-PS in the square conguration NC3, showing the result of Fig. 5.8. It can be immediately seen that the performance gap between the sub-optimal strategies and the optimal benchmark is very small. The maximum gap arises when L-RA with ASub-PS solution is exploited, but leading only to loss of 0.12 bits/s/Hz. In the case, instead, of L-RA joined to Sub-PS, the loss is even less. The trend of the curves is exactly as we expected because the L-RA with Sub-PS strategy evaluates the RA for each link, considering the end-to-end GP only during the path selection step while in the case of L-RA, ASub-PS strategy, the path with the minimum PER sum is selected, without considering the end-to-end GP. In other words, the ASub-PS criterio does not consider the transmission time of a packet from the source to the receiver. Therefore, L-RA with Sub-PS offers an excellent solution with a computational complexity $\mathcal{O}(M^3)$ compared to the optimal one O-RA, O-PS. The L-RA, ASub-PS method, moreover, is a good compromise between AGP performance and computational complexity that is equal to $\mathcal{O}(M^2)$. The result of Fig. 5.9 verifies the efficiency of the LPP method based on kESM technique (2.2) that is exploited to dene PGP function and A-PGP one. This result is shown for a multihop transmission in the generic random conguration NC4. In this scenario the RNs and the PU are randomly positioned before starting the transmission of the packets and then they maintain the position for each value of P_{tot}. RNs and PU can be placed in the area delimited by the square with perimeter

of color blue and green respectively. As we can see, PGP and A-PGP perfectly predict the AGP performance of the transmission. Therefore, the transmission parameters, $\mathbf{P}_l$ and ϕ_l $\forall l \in \mathcal{L}$, are correctly chosen by the O-RA and L-RA algorithms.

Always with reference to the scenario with random position of relays and PU, another interesting simulation shows the AGP performance for the proposed RA and PS methods, fixing the maximum number of RNs $L_{\max}$ at 2, 3 or 4 in the multihop transmission. Therefore, the constraint $0 \leq L \leq L_{\max} \leq M$ is considered. Here too, the performance gap has remained unchanged, as in Fig. 5.8. and only a slight deterioration of the ASub-PS method for $L \leq 2$ has been registered, most likely due to the reduction of possible path form ST to SR. This performance is show in Figure 5.10. Thus, the proposed methods L-RA with Sub-PS and ASub-PS are definitively confirmed as a good solution for RA and PS in a multi-hop transmission because reducing at the same time signaling over the feedback channel and computational complexity. Finally, it should be noted that for $L \leq 3$ the AGP performance is practically identical to that obtained with $L \leq 4$. As a consequence, this result leads to the further and unexpected conclusion that it makes little sense to increase indenitely the number of RNs to ensure that the packet reaches the SR. For to strengthen this conclusion we have increased the number of RNs in NC4 up to 10 and fixed the available power P to 16 and 26 dBm. The distance between any two nodes has been fixed to 40 m and the number of transmitted packet $N_{pck} = 500$. In Figure 5.11 is show as already after two or three relay there isn't any significant improvement! The same can be said for the Figure 5.12. We can concluded that to growing of RNs, also the transmission time of the packet increases and, therefore, the AGP does not improve.

BIC-OFDM and Channel Parameters	*Value*
Information bits (N_{p})	1024
CRC (N_{CRC})	32
Subcarriers (N)	1320
FFT size (N_{fft})	2048
Bandwidth (B)	20 MHz
Cyclic prefix (ν)	160
4-, 16-, 64-QAM modulation ($m_n \; \forall n \in \mathcal{N}$)	2, 4, 6
Convolutional code with rate (r)	1/2, 2/3, 3/4, 5/6
Noise in OFDM bandwidth ($N_0 \cdot N$)	-100 dBm
Doppler frequency (f_{d})	144 Hz
CSI update interval (D)	7
Memory of the predictor (P)	4
Estimation error (σ_e^2)	N_0/S
Interference threshold ($\mathcal{I}_1/\sigma_w^2$)	50 dB

Table 5.1: System parameters

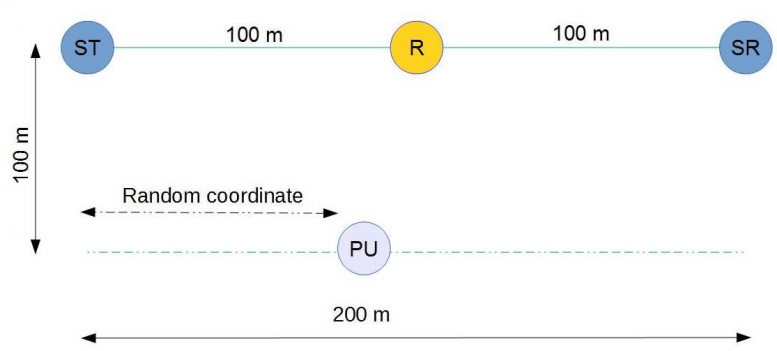

Figure 5.1: C1, line conguration with M = 1 RN

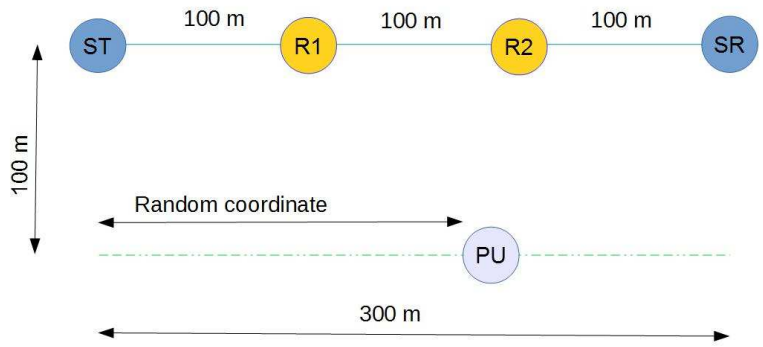

Figure 5.2: C2, line configuration with $M = 2$ RNs

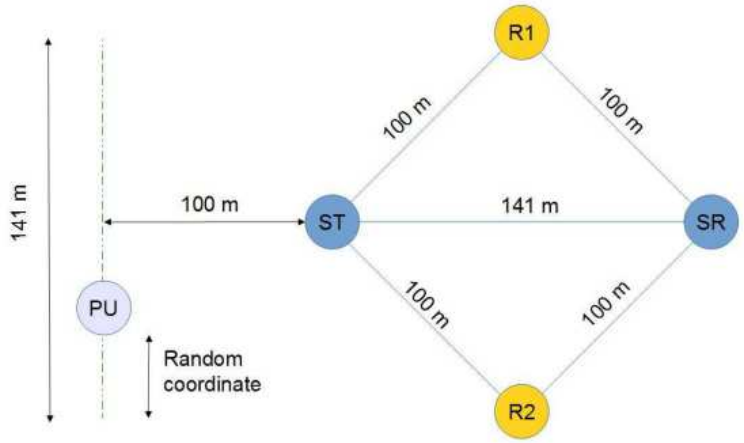

Figure 5.3: Square configuration with $M = 2$ RNs and direct link

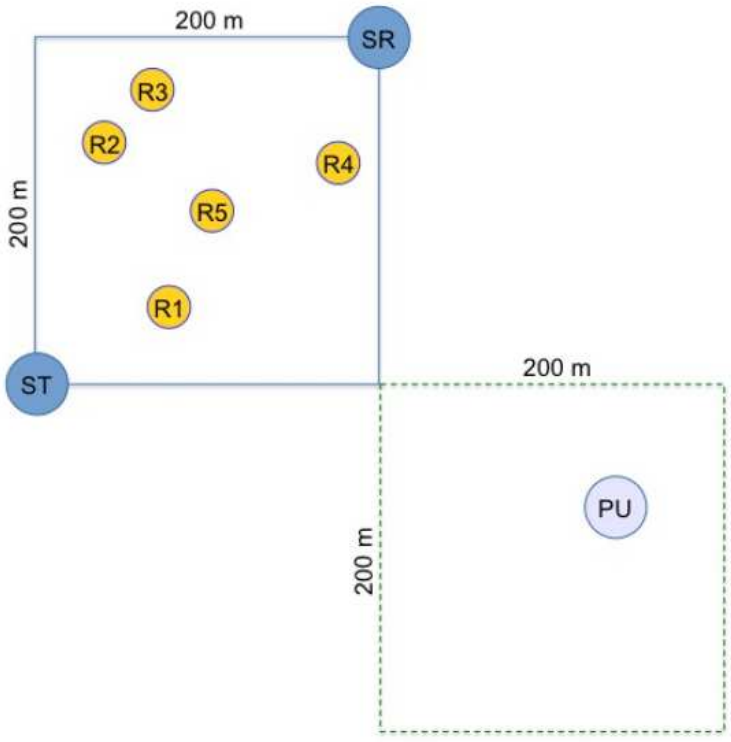

Figure 5.4: NC4, random conguration with M = 5 RNs and direct link

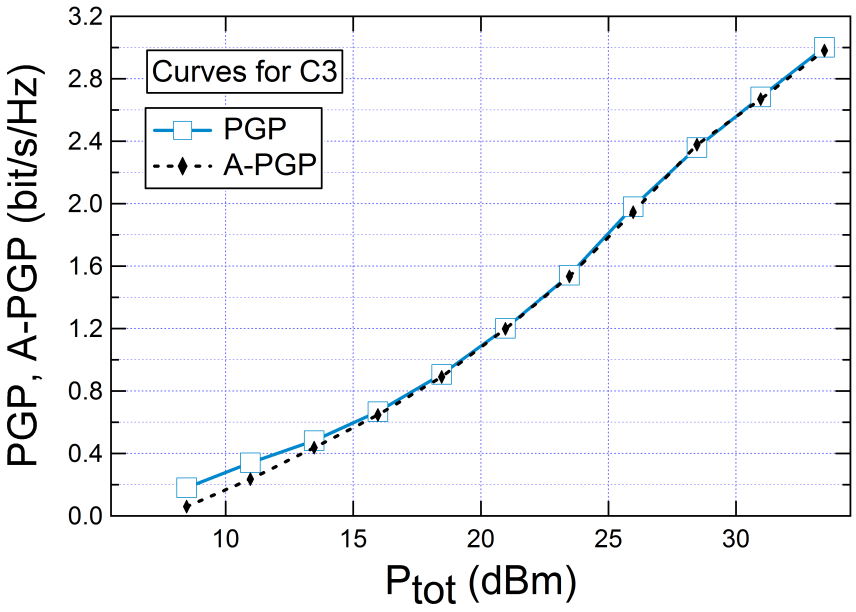

Figure 5.5: Predicted goodput approx average goodput

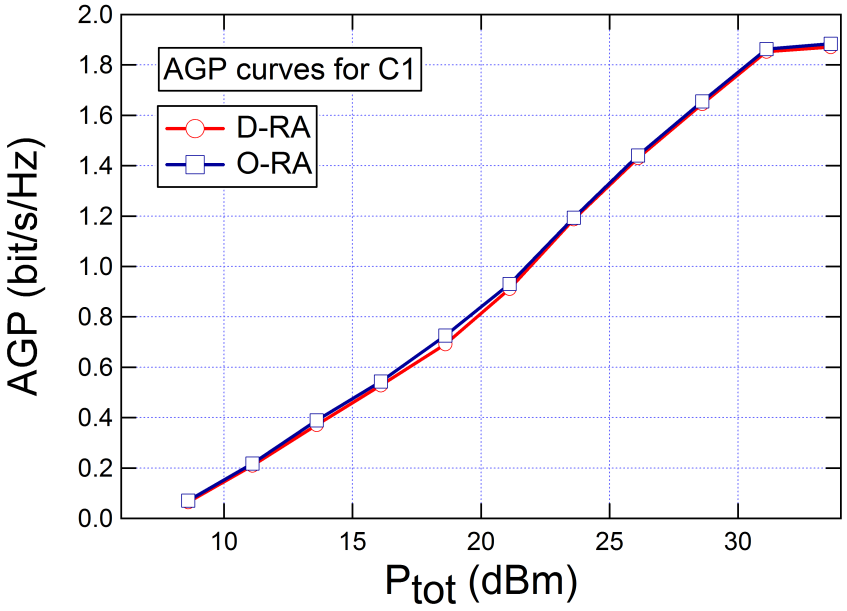

Figure 5.6: AGP comparison in NC1 conguration

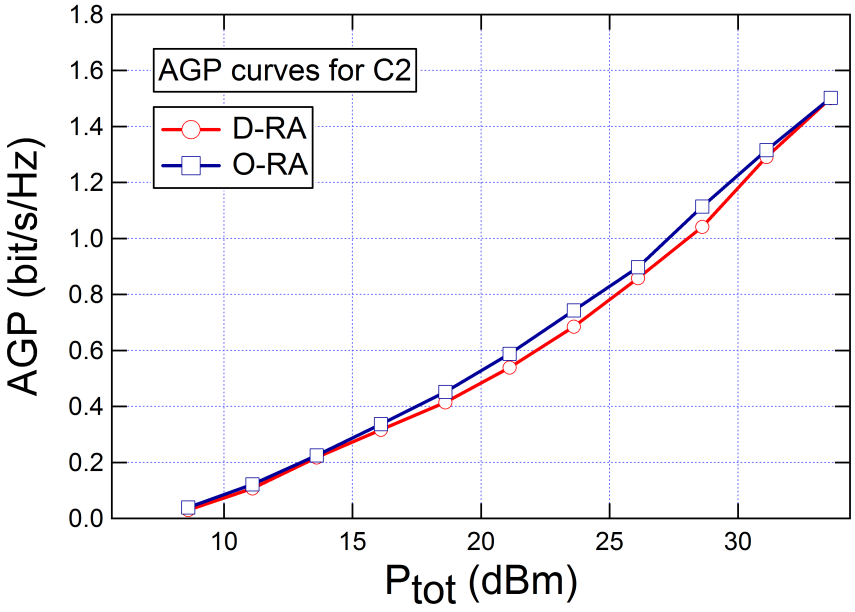

Figure 5.7: AGP comparison in NC2 conguration.

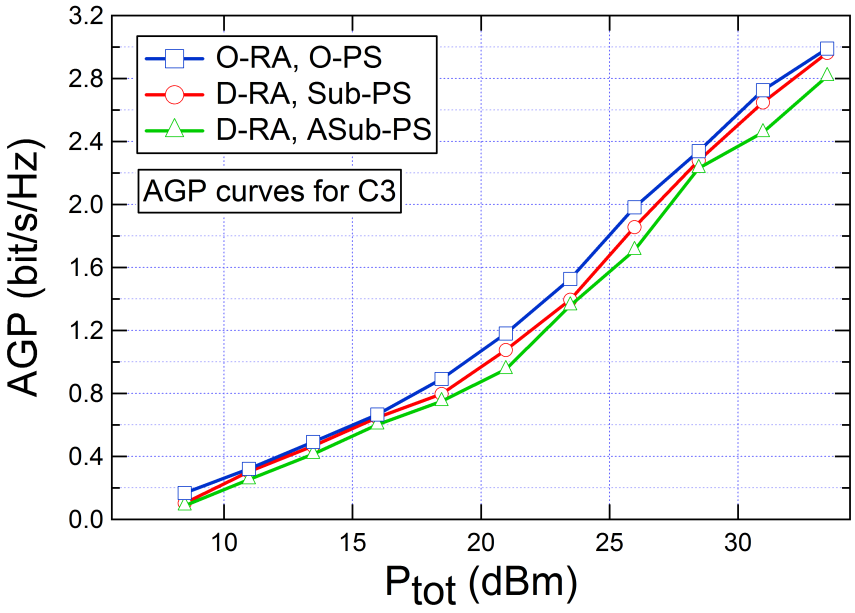

Figure 5.8: AGP comparison in NC3 square conguration

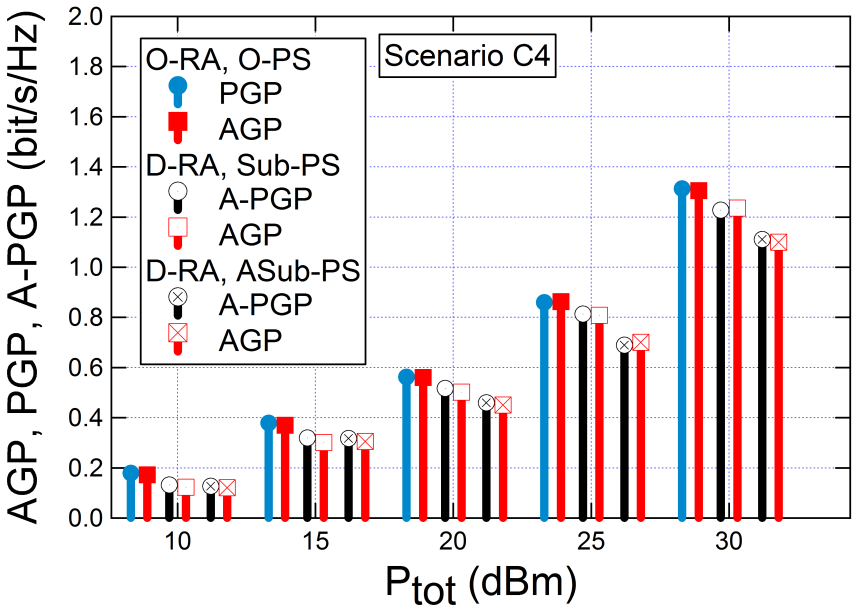

Figure 5.9: PGP, A-PGP and AGP in NC4 random conguration

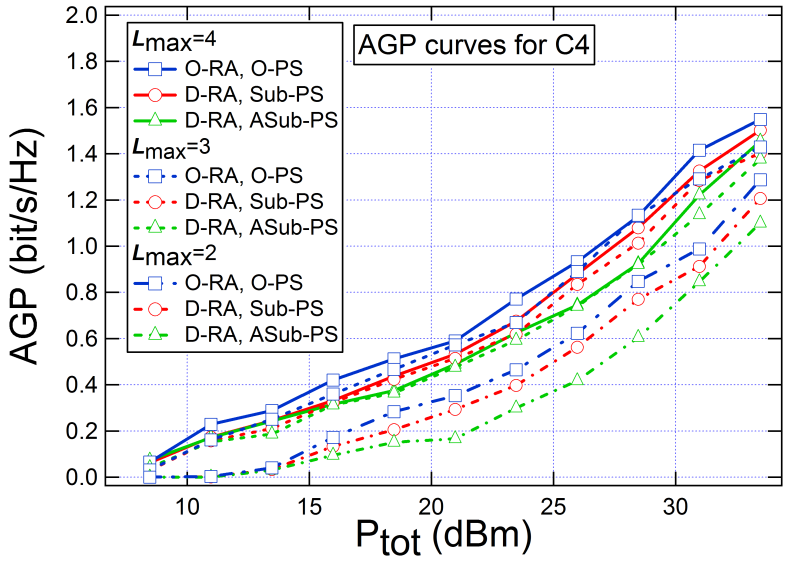

Figure 5.10: AGP comparison in NC4 random conguration

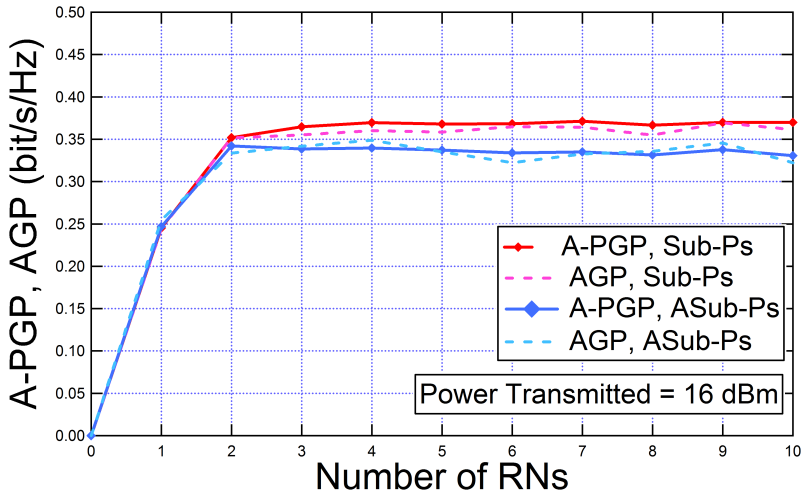

Figure 5.11: A-PGP evolution with variable number of relay

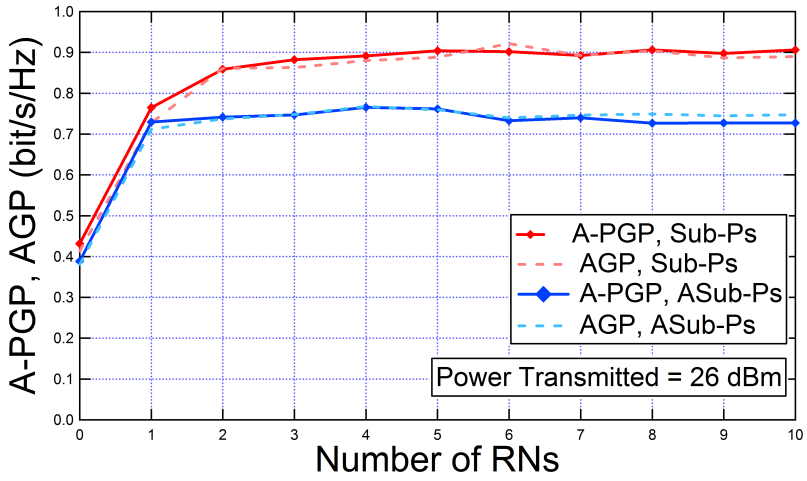

Figure 5.12: A-PGP evolution with variable number of relay

Conclusion

As we have said multihop technique can enhance data rates, coverage and other specific parameters within a network so multihop comunication will be an increasingly important part. In this work we have presented some specific techniques and strategies of RA and PS that are able to reduce the signaling over the feedback channel and the computational complexity. The proposed solutions L-RA with Sub-PS and L-RA with ASub-PS, are able to easily limit the amount of signaling over the feedback channel when RA and PS problems are evaluated among the nodes of the network with a irrelevant loss of GP performance compared with the optimal scheme O-RA, O-PA. Moreover, Sub-PS reduces the computational complexity to $\mathcal{O}(M^3)$ and ASub-PS to $\mathcal{O}(M^2)$. However, ASub-PS problem does not consider the transmission time of a packet, as a consequence, the GP performance is slightly degraded compared to the Sub-PS problem. In this work the GP proves to be an excellent metric to measure the QoS in a multihop network, evaluating the quality of a path as a ratio between probability of correctly receive the information and transmission time. Indeed, we showed in a scenario with ten relays, that the performance does not improve by only increasing the number of RNs to connect transmitter and receiver, because consequently also the transmission time of a packet grows. Therefore, the numerical results make a clear point on the fact that L-RA with Sub-PS or ASub-PS can be applied in a real packed-oriented multihop communication with

practical modulation and coding schemes.

Bibliography

[1] ITU towards IMT for 2020 and beyond? "http://www.itu.int/en/ITU-R/study-groups/rsg5/rwp5d/imt-2020/Pages/default.aspx".

[2] Thompson, J.; Ge, X.; Wu, H.-C.; Irmer, R.; Jiang, H.; Fettweis, G.; Alamouti, S., "5G wireless communication systems: prospects and challenges [Guest Editorial]," Communications Magazine, IEEE, vol.52, no.2, pp.62,64, February 2014.

[3] Wang, T.; Cano, A.; Giannakis, G.B.; Laneman, J.N., "High-Performance Cooperative Demodulation With Decode-and- Forward Relays," in Communications, IEEE Transactions on, vol.55, no.4, pp.830-830, Apr. 2007.

[4] Muller, C.; Klein, A.; Wegner, F.; Kuipers, M., "Costs and Performance of Non-Cooperative Relay Networks," Proceedings of the 13th European Wireless Conference, Paris, France, Apr. 2007.

[5] Ying-Dar Lin; Yu-Ching Hsu, "Multihop cellular: a new architecture for wireless communications," in INFOCOM 2000. Nineteenth Annual Joint Conference of the IEEE Computer and Communications Societies. Proceedings. IEEE , vol.3, no., pp.1273-1282 vol.3, 26-30 Mar. 2000.

[6] Pan Li; XiaoXia Huang; Yuguang Fang, "Capacity scaling of multi-hop cellular networks," in INFOCOM, 2011 Proceedings IEEE , vol., no., pp.2831-2839, 10-15 April 2011.

[7] Mikio Iwamura; Hideaki Takahashi; Satoshi Nagata; "Relay technology in LTE-Advanced"

[8] Xiaohu Ge, Senior Member, IEEE; Song Tu Guoqiang Mao, Senior Member, IEEE; Cheng-Xiang Wang, Senior Member, IEEE, Tao Han, Member, IEEE; "5G Ultra-Dense Cellular Networks".

[9] Chukwu Michael .C, "Comparative study and Security Limitations of 4G Network (Case Study LTE and WIMAX)"

[10] Mikio Iwamura, NGMN 5G Initiative Workstream Lead "Technol. e Archit." on behalf of the NGMN Alliance, Frankfurt, Germany

[11] Ying-Dar Lin, Nat. Chiao Tung Univ. (NCTU), Hsinchu, Taiwan; Yu-Ching Hsu ; Mainak Chattterjee ; Thomas Kunz "Multihop cellular: from research to systems, standards, and applications [Guest Editorial]"

[12] Le, L.; Hossain, E.; "Multihop cellular networks: potential gains, research challenges, and a resource allocation framework," IEEE Commun. Mag., vol.45, no.9, pp.66,73, Sept. 2007.

[13] Pabst, R.; Walke, B.H.; Schultz, D.C.; Herhold, P.; Yanikomeroglu, H.; Mukherjee, S.; Viswanathan, H.; Lott, M.; Zirwas, W.; Dohler, M.; Aghvami, H.; Falconer, D.D.; Fettweis, G.P., "Relay-based deployment concepts for wireless and mobile broadband radio," Communications Magazine, IEEE, vol.42, no.9, pp.80,89, Sept. 2004.

[14] Seung-Jun Kim; Xiaodong Wang; Madihian, M., "Optimal resource allocation in multi-hop OFDMA wireless networks with cooperative

relay," in Wireless Communications, IEEE Transactions on , vol.7, no.5, pp.1833-1838, May 2008.

[15] Xiaolu Zhang; Meixia Tao; Wenhua Jiao; Chun Sum Ng, "End-to-end outage minimization in OFDM based linear relay networks," in Communications, IEEE Transactions on , vol.57, no.10, pp.3034-3044, Oct, 2009.

[16] Chao-Fang Shih; Wanjiun Liao; Hsi-Lu Chao, "Joint Routing and Spectrum Allocation for Multi-Hop Cognitive Radio Networks with Route Robustness Consideration," in Wireless Communications, IEEE Transactions on , vol.10, no.9, pp.2940-2949, Sept. 2011.

[17] Jia Liu; Shroff, N.B.; Sherali, H.D., "Optimal Power Allocation in Multi-Relay MIMO Cooperative Networks: Theory and Algorithms," in Selected Areas in Communications, IEEE Journal on , vol.30, no.2, pp.331-340, Feb. 2012.

[18] Mondelli, M.; Qi Zhou; Lottici, V.; Xiaoli Ma, "Joint Power Allocation and Path Selection for Multi-Hop Noncoherent De- code and Forward UWB Communications," Wireless Communications, IEEE Transactions on , vol.13, no.3, pp.1397,1409, March 2014.

[19] Van Hecke, J.; Del Fiorentino, P.; Andreotti, R.; Lottici, V.; Giannetti, F.; Vandendorpe, L.; Moeneclaey M.; "Goodput-maximizing Resource Allocation in Cognitive Radio Multi-hop BIC-OFDM systems" Communications (ICC), 2015 IEEE International Conference on , June 2015.

[20] Bhushan, N.; Junyi Li; Malladi, D.; Gilmore, R.; Brenner, D.; Damnjanovic, A.; Sukhavasi, R.; Patel, C.; Geirhofer, S.; "Network densication: the dominant theme for wireless evolution into 5G"

Communications Magazine, IEEE, vol.52, no.2, pp.82,89, February 2014.

[21] Lingyang Song; Niyato, D.; Zhu Han; Hossain, E., "Game-theoretic resource allocation methods for device-to-device communication" in Wireless Communications, IEEE , vol.21, no.3, pp.136-144, June 2014.

[22] I. Stupia, V. Lottici, F. Giannetti, and L. Vandendorpe, "Link resource adaptation for multiantenna bit-interleaved coded multicarrier systems" IEEE Transactions on Signal Processing, vol. 60, no. 7, pp. 3644 3656, July 2012.

[23] Del Fiorentino, P.; Jeroen Van Hecke; Vincenzo Lottici; Filippo Giannetti; Marc Moeneclaey; "Goodput-based Resource Allocation and Path Selection for Cognitive Radio BIC-OFDM systems," March 28, 2016.

[24] F. Rusek et al., "Scaling Up MIMO: Opportunities and Challenges with Very Large Arrays," IEEE Sig. Proc.Mag., vol. 30, no. 1, Jan. 2013, pp. 4060.

[25] X. Hong et al., "Capacity Analysis of Hybrid Cognitive Radio Networks with Distributed VAAs" IEEE Trans.

[26] J. Mitola. Cognitive Radio: An Integrated Agent Architecture for Software Dened Radio. PhD Dissertation, KTH, Stockholm, Sweden, December 2000.

[27] Federal Communications Commission Spectrum Policy Task Force. Report of the Spectrum Efciency Working Group. Technical Report 02-135, (November), 2002. Download available at http://www.fcc.gov/sptf/les/SEWGFinalReport 1.pdf.

[28] R. Brodersen, A. Wolisz, D. Cabric, S. M. Mishra, and D. Willkomm. CORVUS: A cognitive radio approach for usage of virtual unlicensed spec- trum. White Paper: Berkeley Wireless Research Center. Download available at http://bwrc.eecs.berkeley.edu/research/mcma/CR White paper nal1.pdf.

[29] Shared Spectrum Company. Comprehensive Spectrum occupancy measure- ments over six different locations. August 2005. Download available at http://www.sharedspectrum.com/?section=nsf summary.

[30] Ultra-wideband wireless communications theory and applications. In IEEE J.Select. Areas Commun., vol. 24, no. 4, April 2006.

[31] A. Ghasemi and E. S. Sousa, "Fundamental limits of spectrum-sharing in fading environments," Wireless Communications, IEEE Transactions on, vol. 6, no. 2, pp. 649 658, feb. 2007.

[32] Z. Shu and W. Chen, "Optimal power allocation in cognitive relay networks under different power constraints," in Wireless Communications, Networking and Information Security (WCNIS), 2010 IEEE International Conference on, june 2010, pp. 647 652.

[33] S. Loyka, G. Levin, On Outage Probability and Diversity-Multiplexing Tradeoff in MIMO Relay Channels, IEEE Trans. Comm., v. 59, N. 6, June 2011.

[34] Georgy Levin and Sergey Loyka, Amplify-and-Forward Versus Decode-and-Forward Relaying: Which is Better?

[35] M.-O. Pun, M. Morelli, and C.-C. J. Kuo, Multi-Carrier Techniques for Broadband Wireless Communications. A Signal Processing Perspective. Imperial College Press, London, UK, 2007

[36] J. G. Proakis, Digital Communications, 4th ed. New York, NY: McGraw- Hill, 2001.

[37] J. Proakis, Digital Communications, ser. McGraw-Hill series in electrical and computer engineering. McGraw-Hill Higher Education, 2001. [Online]. Available: http://books.google.be/books?id=sbr8QwAACAAJ

[38] W. C. Jakes, Microwave Mobile Communications. New York: Wiley,1974.

[39] Van Hecke, J.; Del Fiorentino, P.; Giannetti, F.; Lottici, V.; Vandendorpe, L.; Moeneclaey, M., "Resource allocation for multicarrier cooperative cognitive radio networks with imperfect channel state information," in Personal, Indoor, and Mobile Radio Communication (PIMRC), 2014 IEEE 25th Annual International Symposium on , vol., no., pp.653-658, 2-5 Sept. 2014.

[40] Ghasemi, A.; Sousa, E.S.; "Fundamental limits of spectrum-sharing in fading environments," Wireless Communications, IEEE Transactions on, vol.6, no.2, pp.649,658, Feb. 2007.

[41] P. Ciacci, "Bit loading for next generation wireless OFDM systems: a "greedy" approach for goodput optimization", University of Pisa, Department of Information Engineering, Masters Thesis in Telecommunication Engineering, 20 July 2009.

[42] A. Guillen i Fabregas, A. Martinez, and G. Caire, "Bit-interleaved coded modulation," Foundations and Trends in Communications and Information Theory, 2008.

[43] S. Boyd and L. Vandenberghe, "Convex optimization" Cambridge Univ. Press, 2004.

[44] Andreotti, R.; Stupia, I; Lottici, V.; Giannetti, F.; Vandendorpe, L., "Goodput-Based Link Resource Adaptation for Reliable Packet Transmissions in BIC-OFDM Cognitive Radio Networks," Signal Processing, IEEE Transactions on , vol.61, no.9, pp.2267,2281, May1, 2013.

[45] Guerin, R.; Orda, A., "Computing shortest paths for any number of hops" Networking, IEEE/ACM Transactions on , vol.10, no.5, pp.613,620, Oct 2002.

[46] I. Wong and B. Evans, "Optimal resource allocation in the ofdma downlink with imperfect channel knowledge", Communications, IEEE Transactions on, vol. 57, no. 1, pp. 232241, January 2009.

[47] "3GPP TR 25.890 V1.0.0 (2002-05)", pp. 16.

[48] IEEE 802.16m Evaluation Methodology Document (EMD), "IEEE 802.16m-08/004r2," pp. 143, July 2008.

Ringraziamenti